SAND2018-3061C

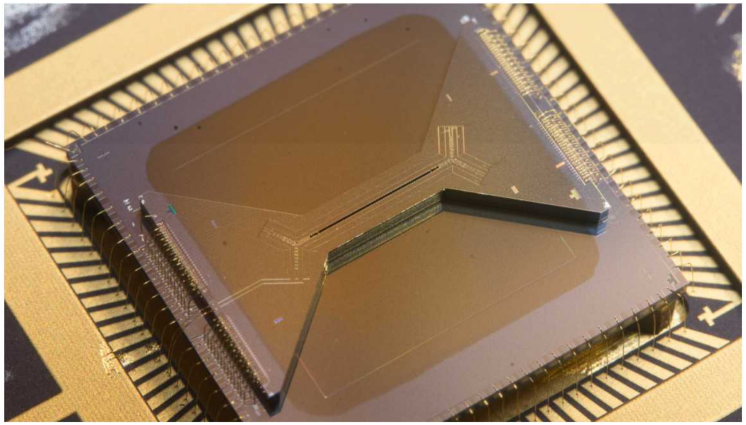

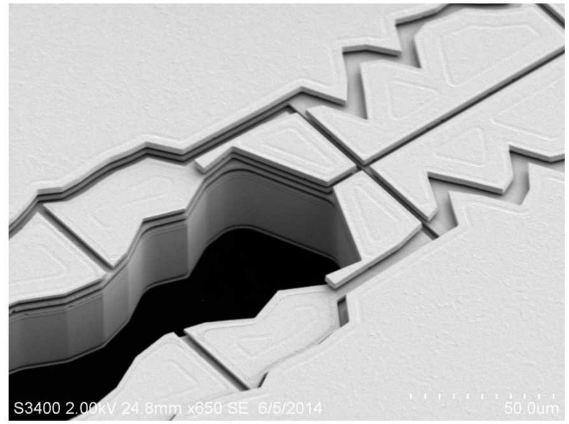

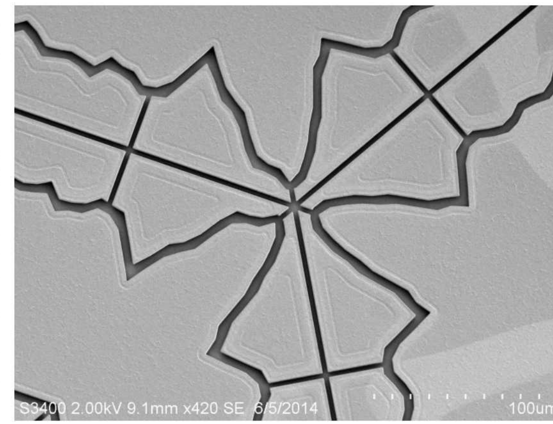

Surface ion traps for quantum computing

NPQI 2018

Daniel Stick, Sandia National Laboratories

P. Maunz, M. G. Blain, D. Lobser, M. Revelle, C. Yale,

R. Haltli, C. Hogle, A. Hollowell

Sandia National Laboratories is a multimission laboratory managed and operated by National Technology & Engineering Solutions of Sandia, LLC, a wholly owned subsidiary of Honeywell International, Inc., for the U.S. Department of Energy's National Nuclear Security Administration under contract DE-NA0003525.

Outline

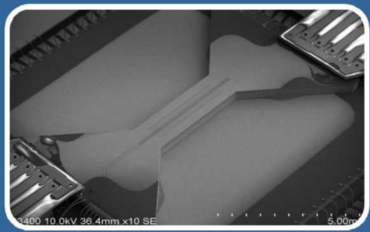

Trap fabrication, advantages and challenges

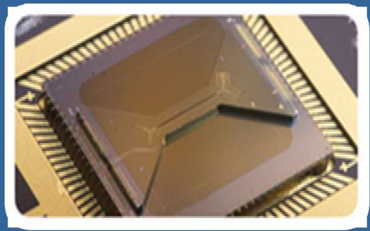

Recent trap types: High Optical Access trap & Microwave trap

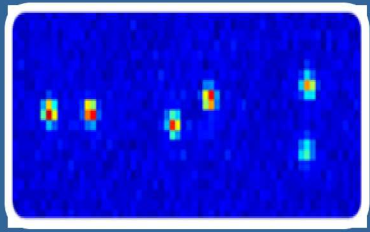

Ion shuttling and swapping

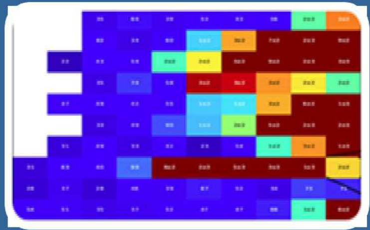

Characterization of quantum gates using Gate Set Tomography (GST)

Advantages/Challenges vs 3D

Advantages

- Greater field control (more electrodes)
- Flexible, precise 2D geometry
- More manufacturable
- Consistent geometry → consistent behavior
- Laser access
- Integration of other technologies (waveguides, detectors, filters…)

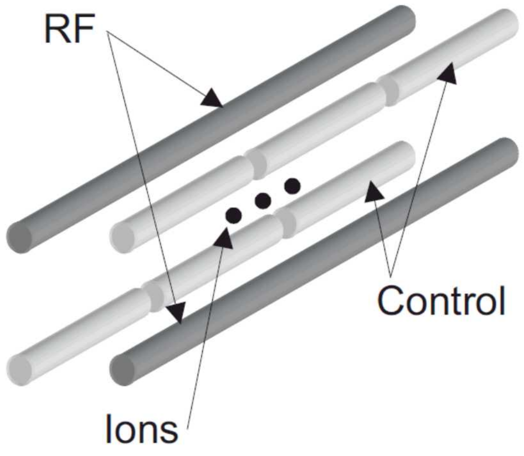

Challenges

- Lower depth (ion lifetime), anharmonicities in potential
- Proximity to surface (charging, heating)
- Delicate (dust, voltage)
- Capacitance
- Laser access

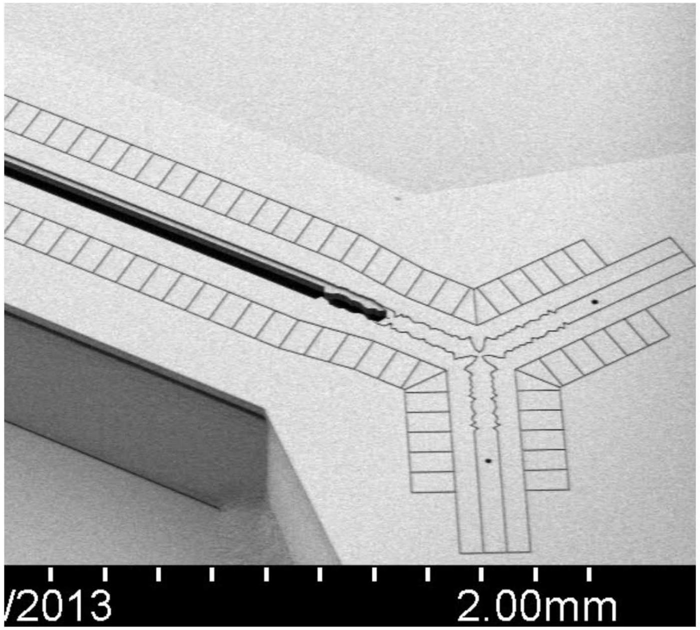

Capabilities & Requirements

Essential capabilities

- Reliable and consistent operation
- Store ions for long periods of time (hours)
- Move ions to achieve 2D connectivity
- Support high fidelity operations

MESA facility

- Radiation hardened CMOS
- Leverages reliability of NW processing
- Large feature sizes (350 nm) match well with trap requirements

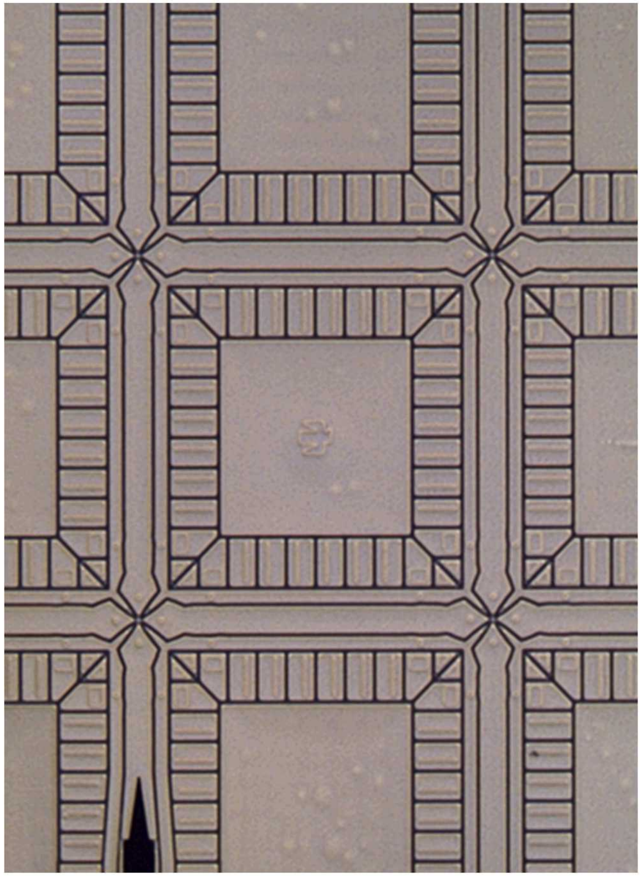

Capabilities & Requirements

Derived requirements

- Standardization (lithographically defined electrodes)
- Multi-unit production
  - ~90 devices per 6" wafer
- Multi-level lead routing for accessing interior electrodes
  - Connecting both control and RF electrodes
- Voltage breakdown >300 V @ ~50 MHz
- Overhung electrodes
- Low electric field noise (heating)
- Backside loading holes
- Trench capacitors
- High optical access (delivery and collection)

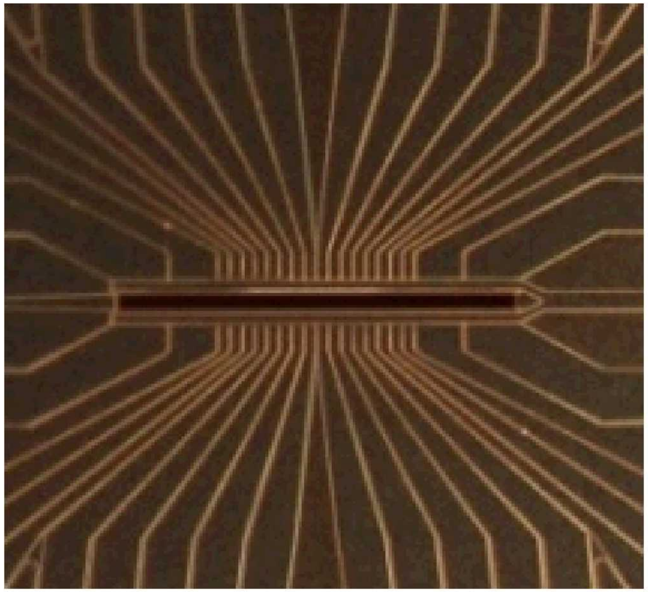

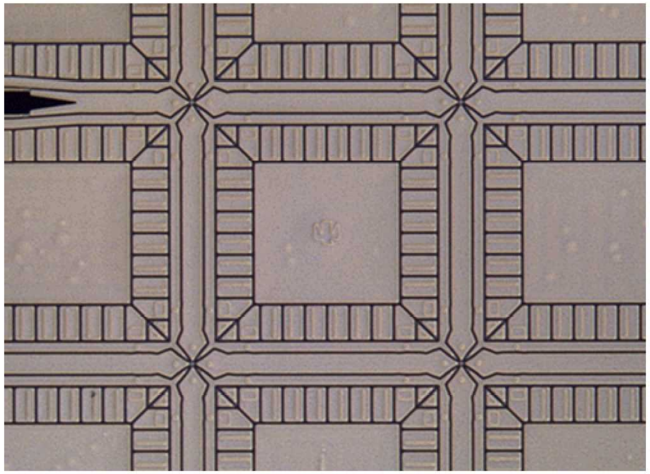

Capabilities & Requirements

Derived requirements

- Standardization (lithographically defined electrodes)
- Multi-unit production
- Multi-level lead routing for accessing interior electrodes
- Voltage breakdown >300 V @ ~50 MHz
- Overhung electrodes
- Low electric field noise (heating)
- Backside loading holes
- Trench capacitors
- High optical access (delivery and collection)

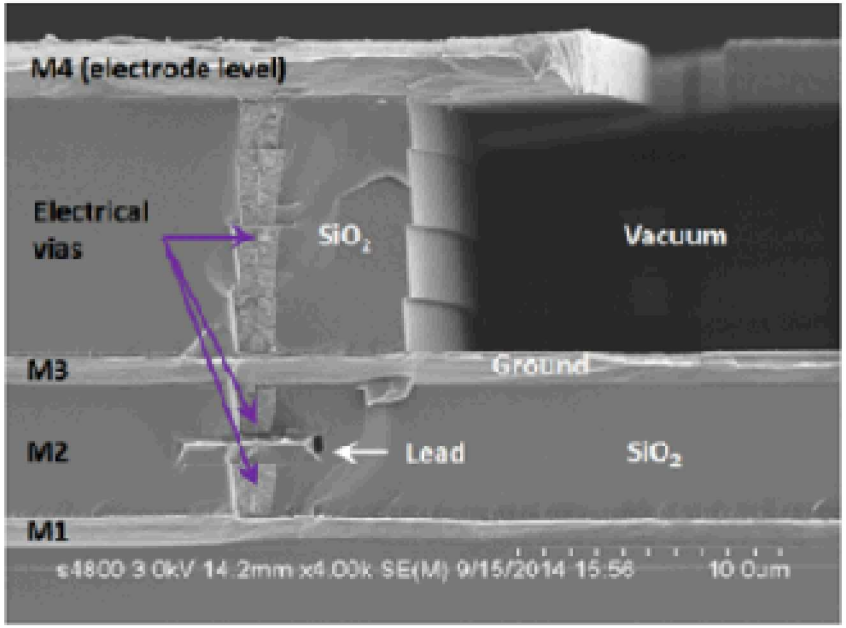

Capabilities & Requirements

Derived requirements

- Standardization (lithographically defined electrodes)
- Multi-unit production
- Multi-level lead routing for accessing interior electrodes
- Voltage breakdown >300 V @ ~50 MHz
- Overhung electrodes
- Low electric field noise (heating)
- Backside loading holes
- Trench capacitors
- High optical access (delivery and collection)

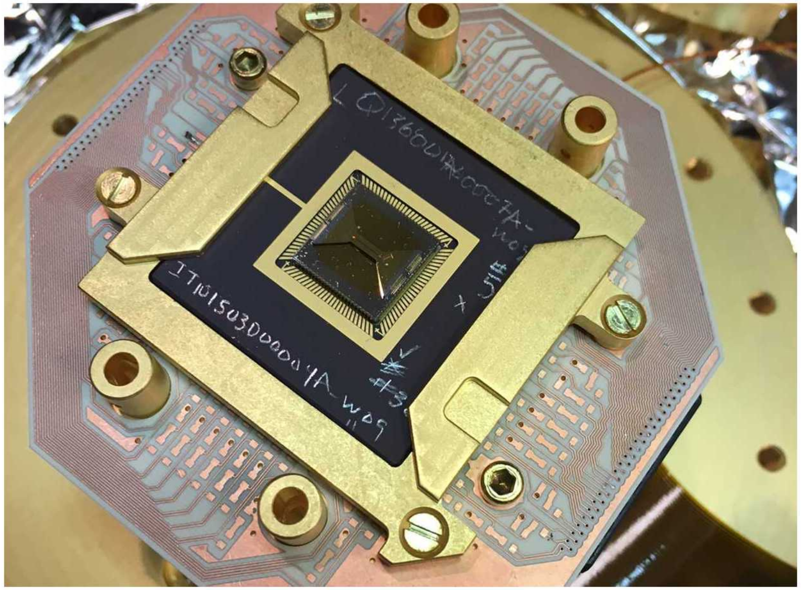

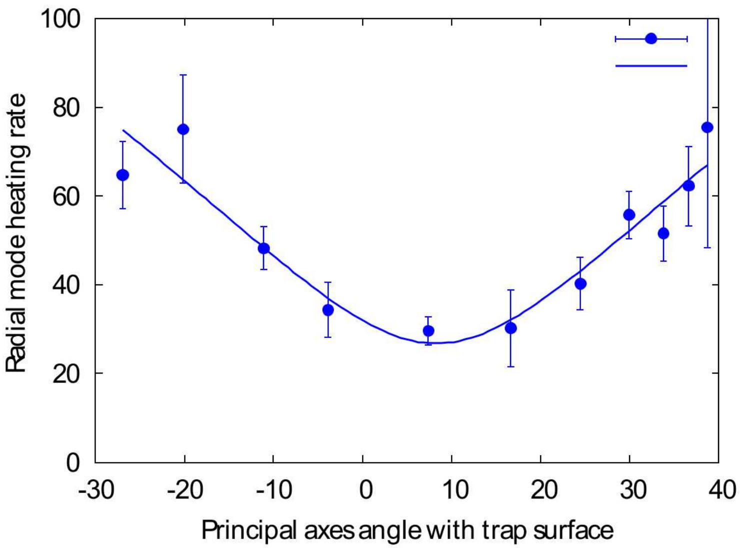

Capabilities & Requirements

Derived requirements

- Standardization (lithographically defined electrodes)
- Multi-unit production
- Multi-level lead routing for accessing interior electrodes
- Voltage breakdown >300 V @ ~50 MHz
- Overhung electrodes
- Low electric field noise (heating)
- Backside loading holes
- Trench capacitors
- High optical access (delivery and collection)

50μm×80μm
modulation necessary

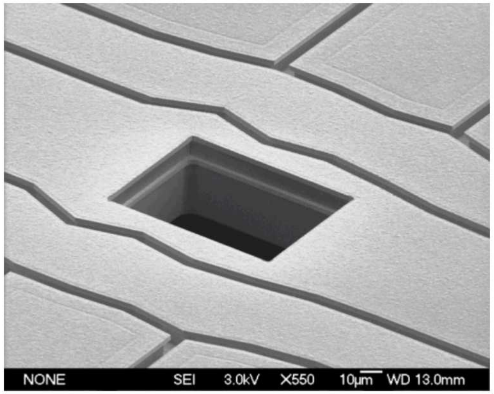

10μm hole
still perturbs the field

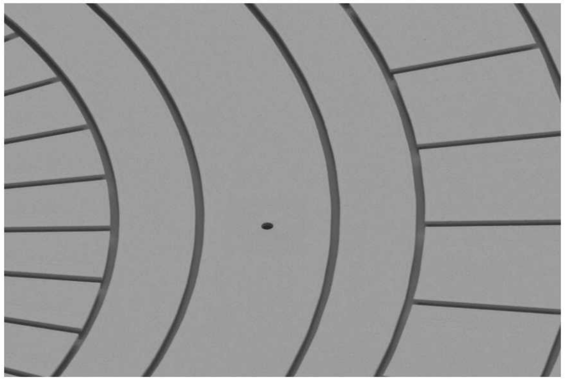

3μm×20μm

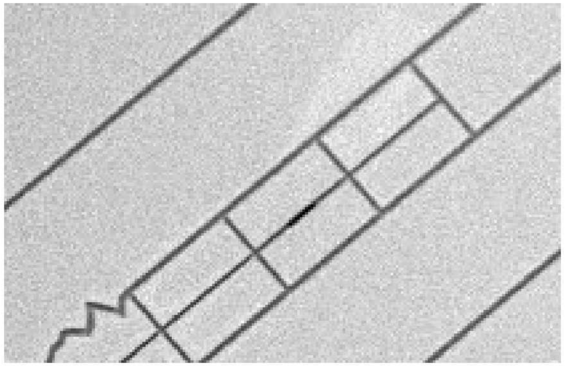

Capabilities & Requirements

Derived requirements

- Standardization (lithographically defined electrodes)
- Multi-unit production
- Multi-level lead routing for accessing interior electrodes
- Voltage breakdown >300 V @ ~50 MHz
- Overhung electrodes
- Low electric field noise (heating)
- Backside loading holes
- Trench capacitors
  - Current: 20V max, 1nF capacitance
  - Future: on-chip, 200 pF capacitance (but low inductance)
- High optical access (delivery and collection)

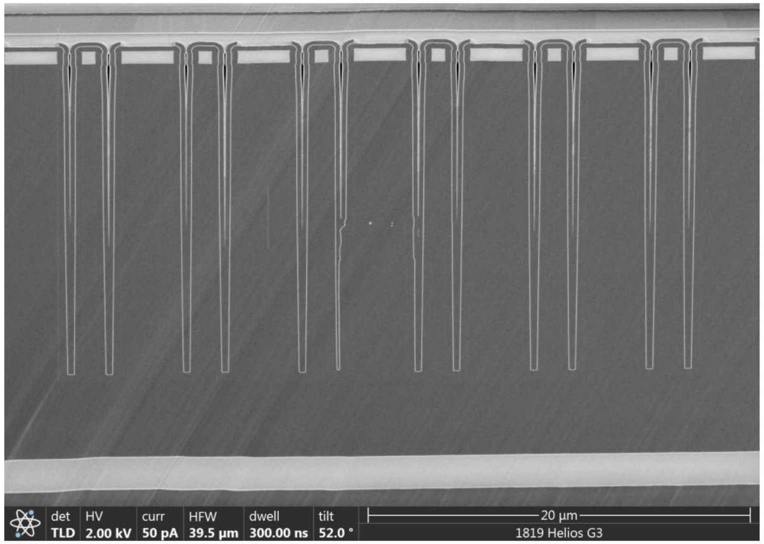

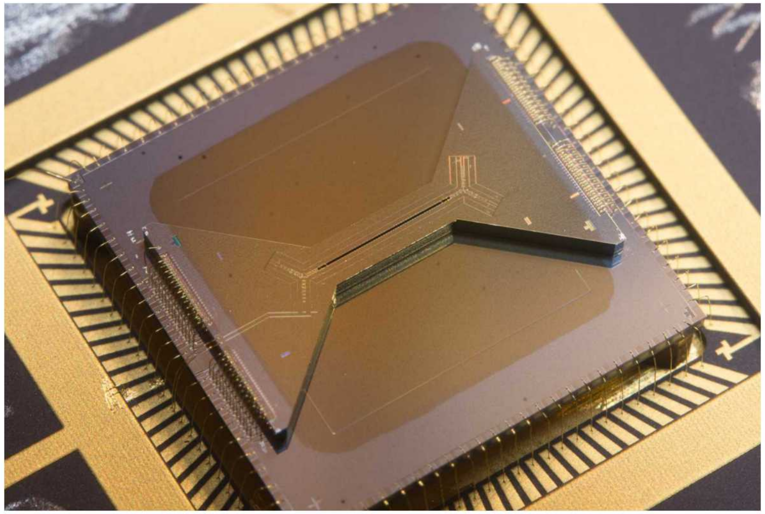

Microwave surface trap

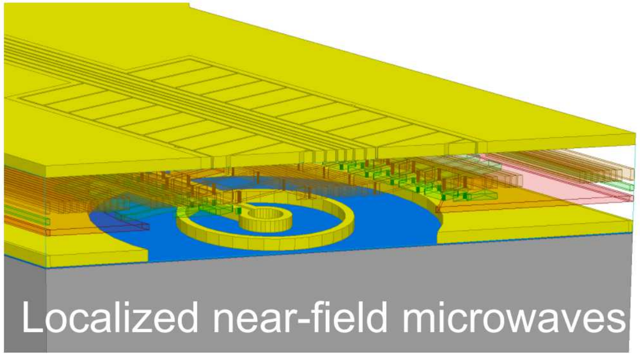

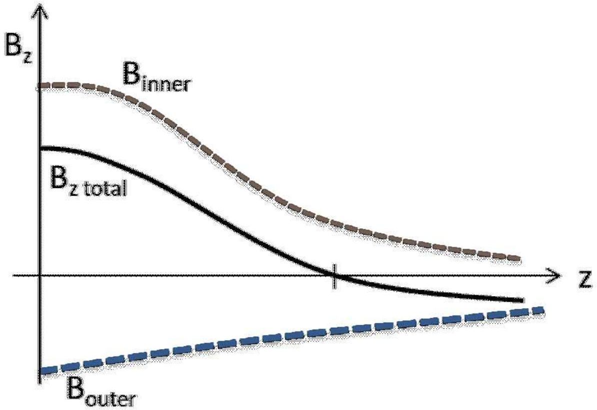

Advantages:

- Microwave radiation is easier to control & cheaper to implement
- Low power for Rabi oscillations
- Near field allows generation of microwave gradient fields

Challenges:

- Microwave delivery (12.6 GHz for Yb)
- Dissipation, heating, thermal management
- Generate both field and gradient

Field characteristics:

- x- and y- fields cancel along z-axis
- Generates uniform B_z and dB_z/dz with B=0
- Location of null determined by geometry & ratio of currents

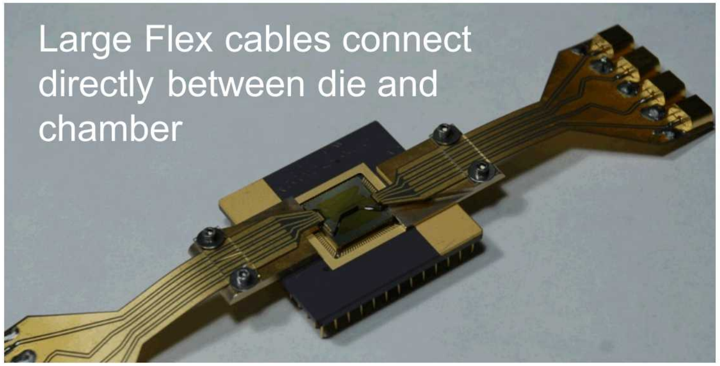

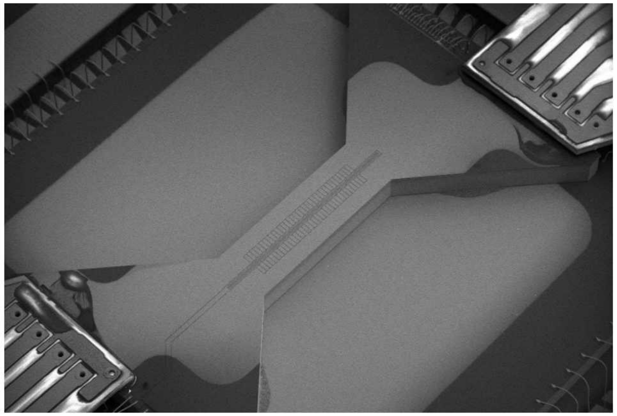

Microwave – single qubit

Fast, efficient Rabi flopping

- Losses between chamber and device ≈17 dB
- Realized fast Rabi flopping
  330 ns with 15 dBm at chamber, -2 dBm at device

Localization

- Microwaves are localized at the loop
- Field suppressed factor 10
- Pickup from the second loop
- Field suppressed factor 5

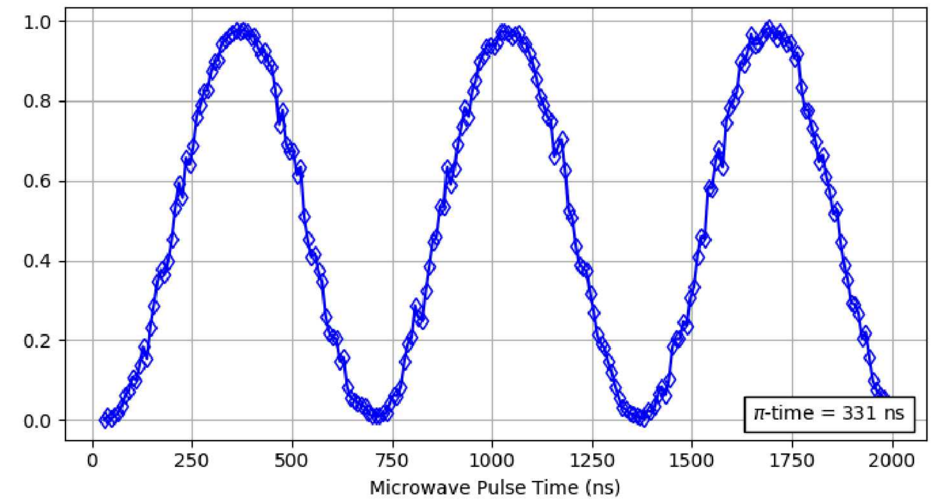

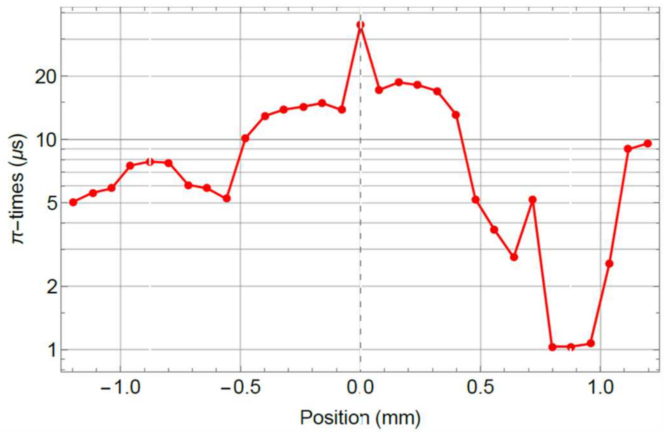

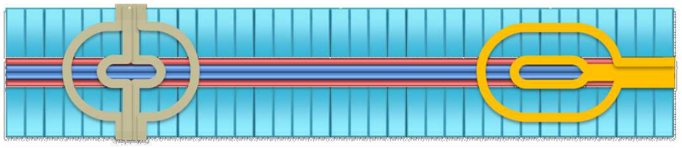

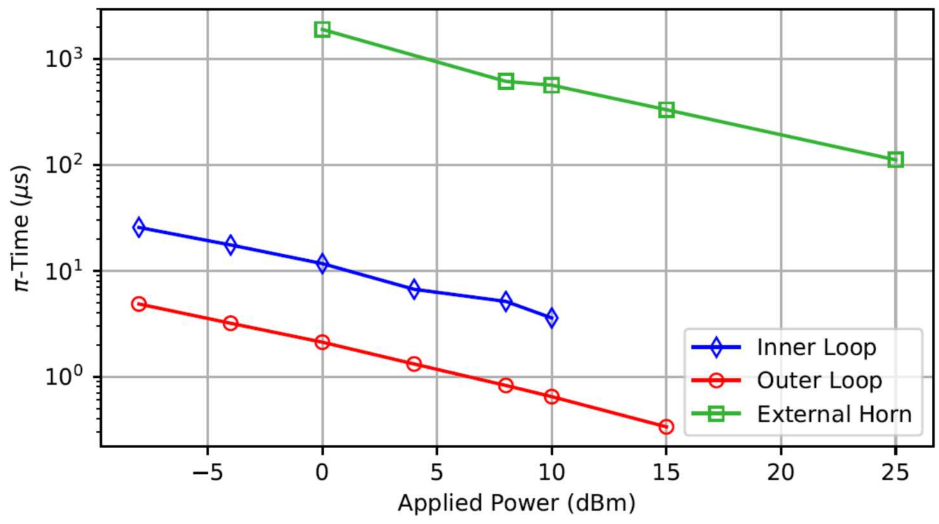

Microwave – motional control

Vertical Mode

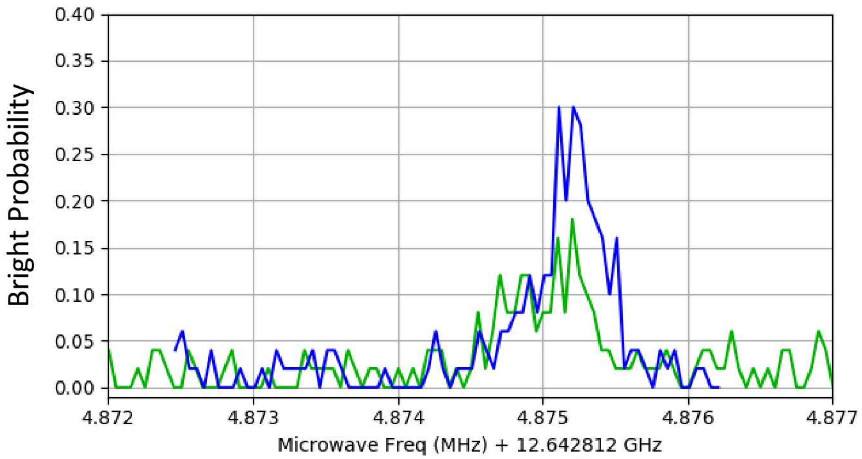

Horizontal Mode

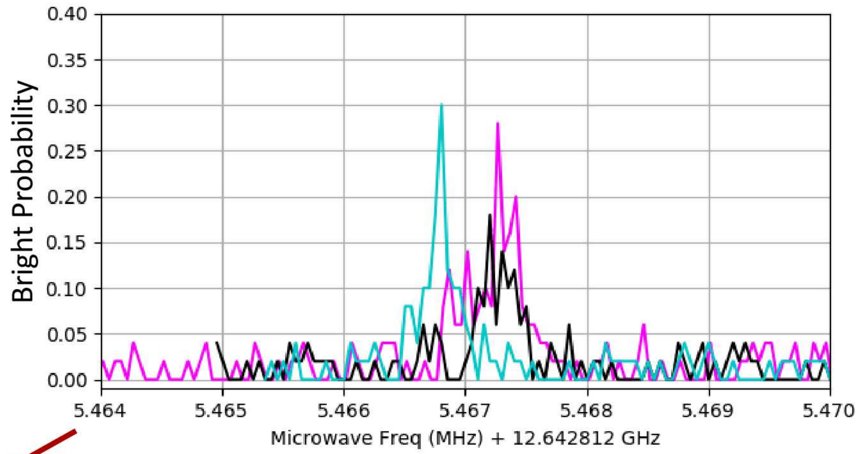

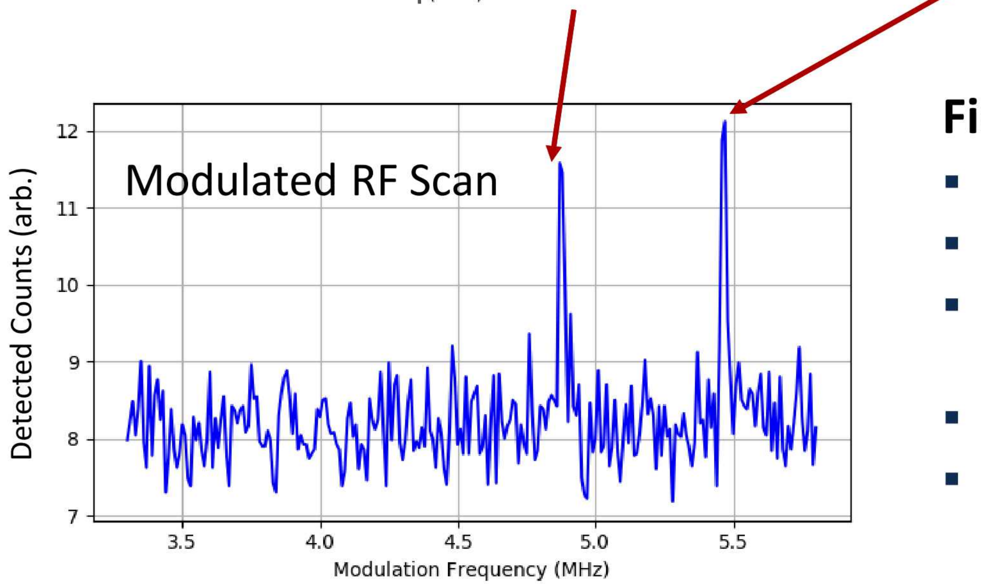

Field characteristics:

- x- and y- fields cancel along z-axis
- Generates uniform B_z and dB_z/dz with B=0
- Location of null determined by geometry and ratio of currents
- Using <20 dBm on each loop
- Measurement time ~ 5 ms

High Optical Access (HOA)

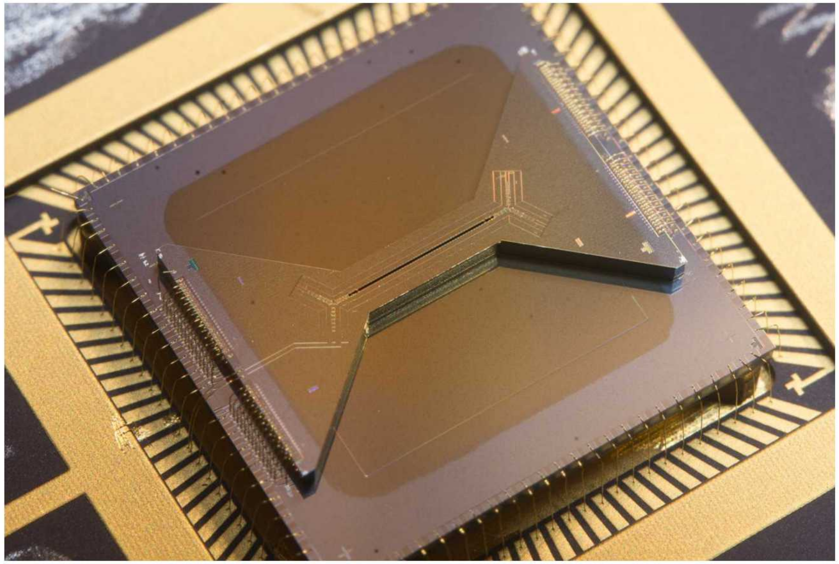

Optical access

- Excellent optical access rivaling 3-D

Trap strength

- Radial trap frequency 2 - 5 MHz
- RF frequency 50 MHz
- Stable for long ion chains
- Low heating rates (30 q/s parallel to surface, 125 q/s perpendicular)
- >100 h observed
  (while running measurements)
- >5 min without cooling

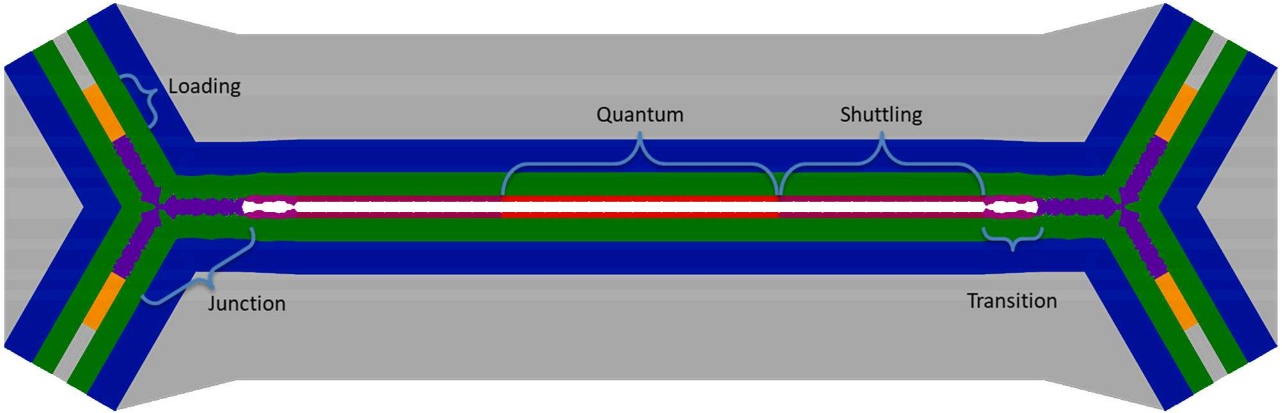

Trapped ion chains

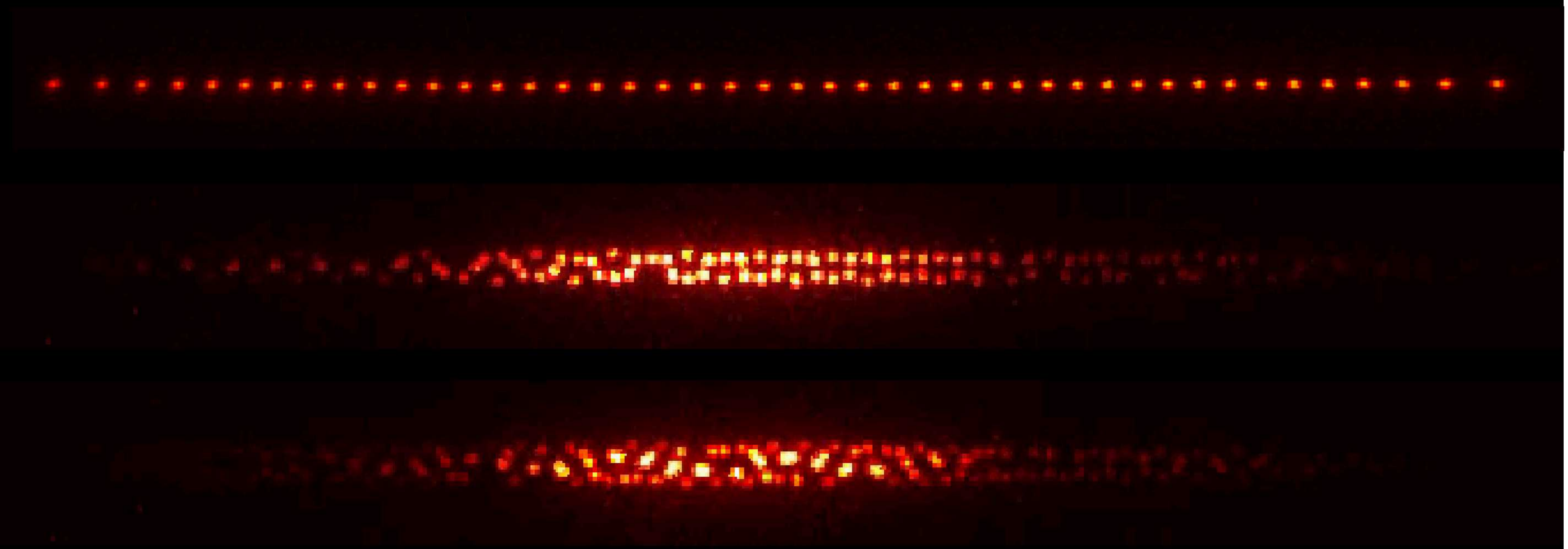

- Observed storage times between
  - 16 min for long linear chain
  - 16 h for 3d crystal
- Most likely limited by background collisions
- Property of vacuum conditions
- Losing all ions at once (one might come back)

HOA control

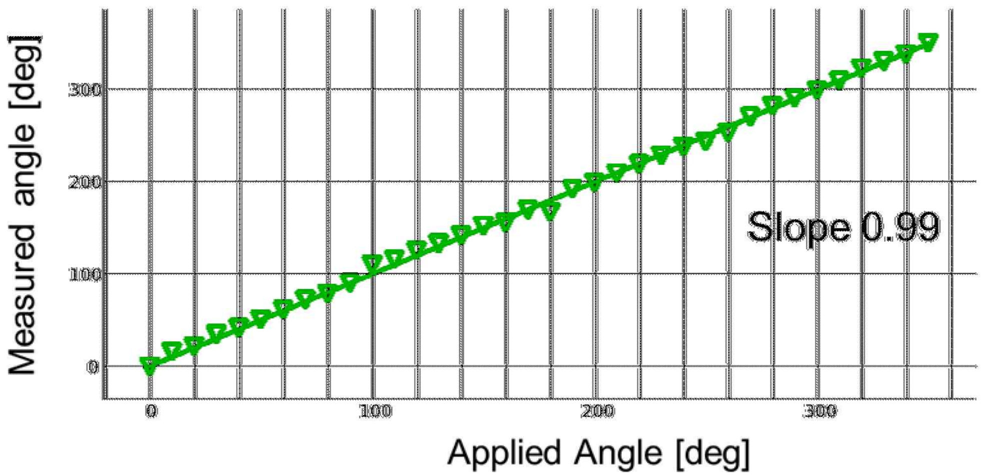

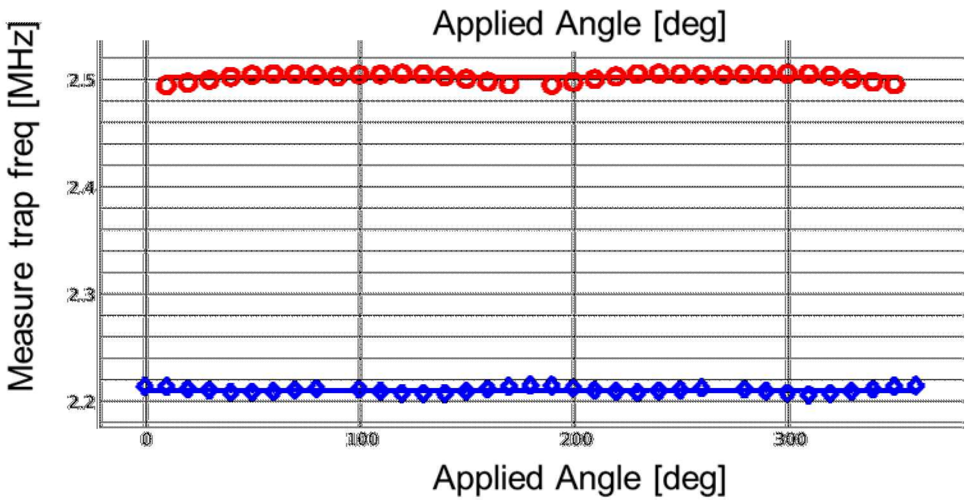

Electric field control

- Do we understand the trapping fields?
- Principal axes rotation realized as in simulation
- No change in trap frequencies
- The simulations accurately describe the fields and curvatures generated by the trap

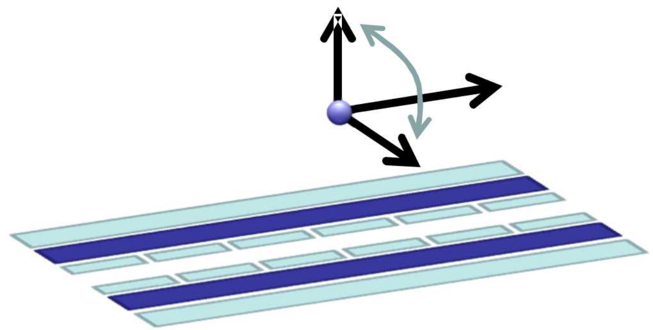

Swapping ions

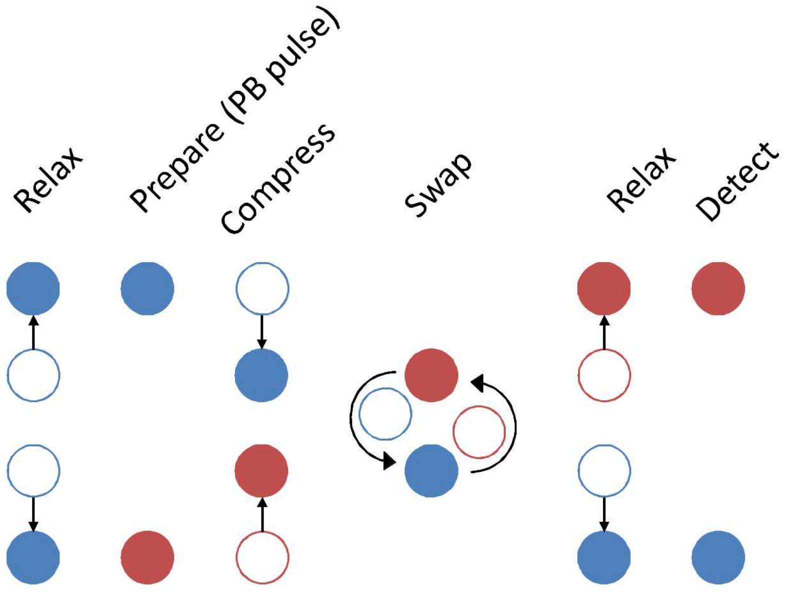

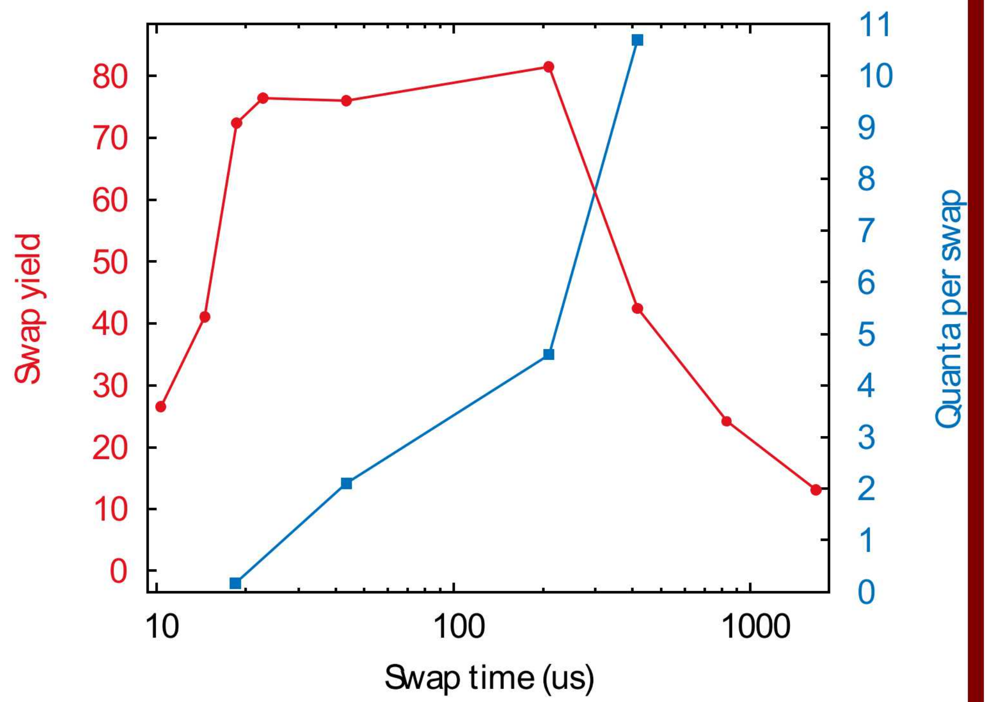

Advantages of parametric trapping solutions:

- Primitives in terms of curvature tensor elements and can be applied at any location in the trap.
- Shuttling primitives can be easily combined
- Example: rotating ion crystal while translating through the trap

Diagnostics - single qubit gate

Gate Set Tomography (GST)

- No calibration required
- Detailed debug information
- Efficiently measures performance characterizing fault-tolerance (diamond norm)
- Amplifies errors
- Detects non-Markovian noise
- Robin Blume-Kohout, Erik Nielsen @ SNL

Desired "target" gates:

G_i	Idle (Identity)
G_x	$\pi/2$ rotation about x-axis
G_y	$\pi/2$ rotation about y-axis

Fiducials:

$\{\}$

Gx

Gy

$Gx \cdot Gx$

$Gx \cdot Gx \cdot Gx$

$Gy \cdot Gy \cdot Gy$

Germs:

Gx

Gy

Gi

$Gx \cdot Gy$

$Gx \cdot Gy \cdot Gi$

$Gx \cdot Gi \cdot Gy$

$Gx \cdot Gi \cdot Gi$

$Gy \cdot Gi \cdot Gi$

$Gx \cdot Gx \cdot Gi \cdot Gy$

$Gx \cdot Gy \cdot Gy \cdot Gi$

$Gx \cdot Gx \cdot Gy \cdot Gx \cdot Gy \cdot Gy$

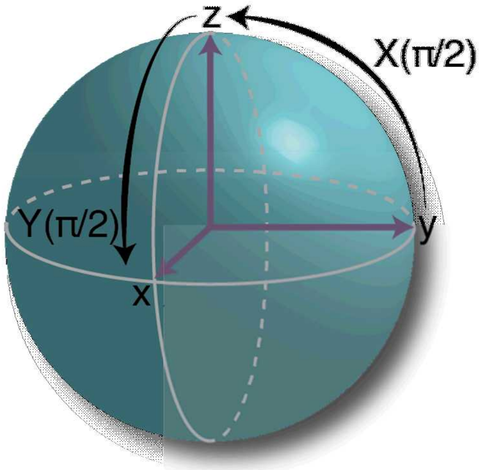

Single qubit BB1 compensated microwave gates on $^{171}Yb^{+}$

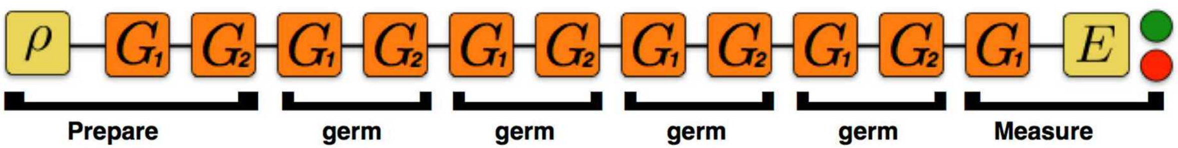

Diagnostics – single qubit gate

GST – Microwaves (horn)

Raw data poor gates

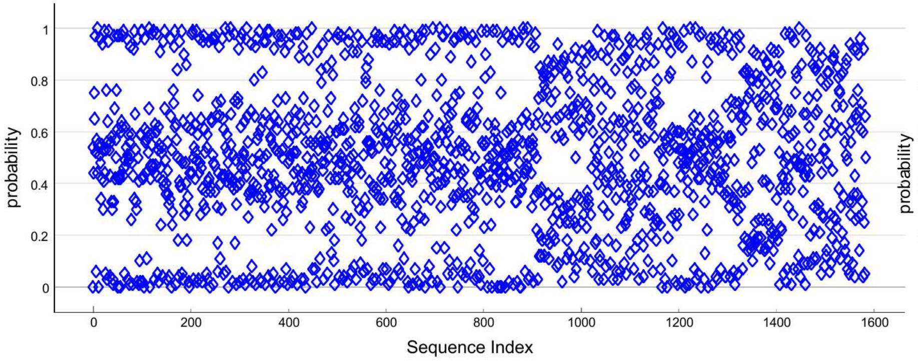

Raw data good gates

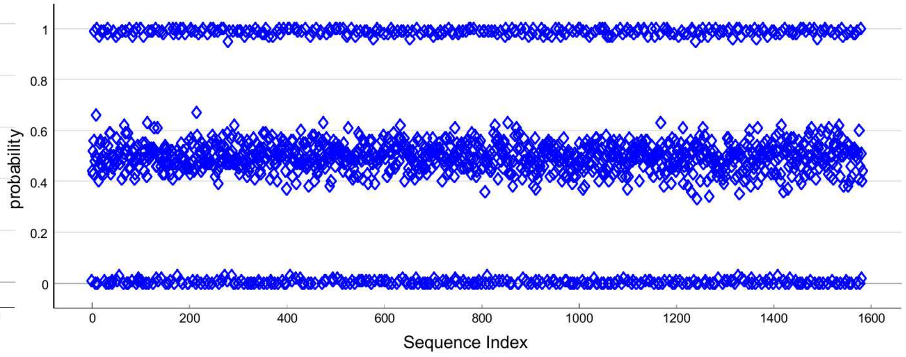

Gate	Rotn. axis	Angle
G_I	0.5252 −0.009 0.8506 −0.0244	0.001699π
G_X	-3×10^{-6} −1 -3×10^{-5} −0.009	0.501308π
G_Y	−0.2474 0.0001 0.9689 −0.0001	0.501366π

Gate	Rotn. axis	Angle
G_I	−0.0035 0.014 −0.9999 0.0006	0.001769π
G_X	-3×10^{-5} −1 1×10^{-4} 0.0006	0.500007π
G_Y	0.1104 4×10^{-5} 0.9939 0.0005	0.50001π

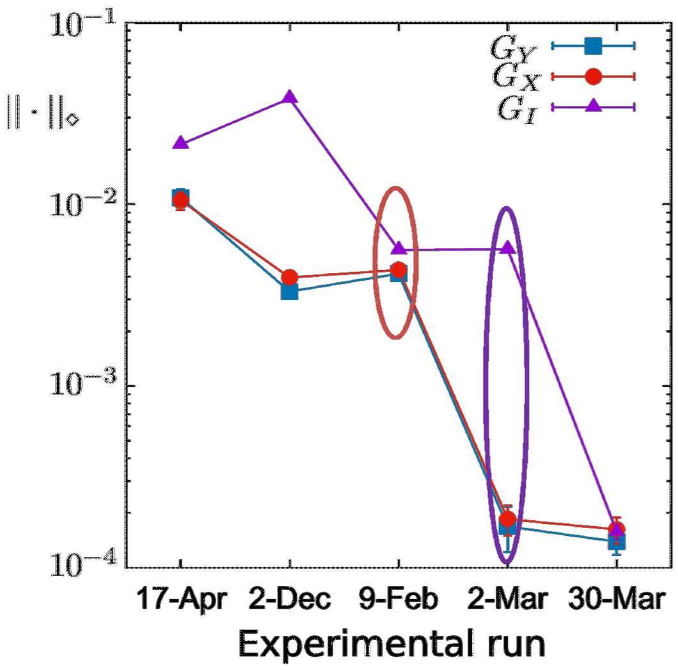

Diagnostics – single qubit gate
GST – Microwaves (horn)

1. Fix switching artifacts

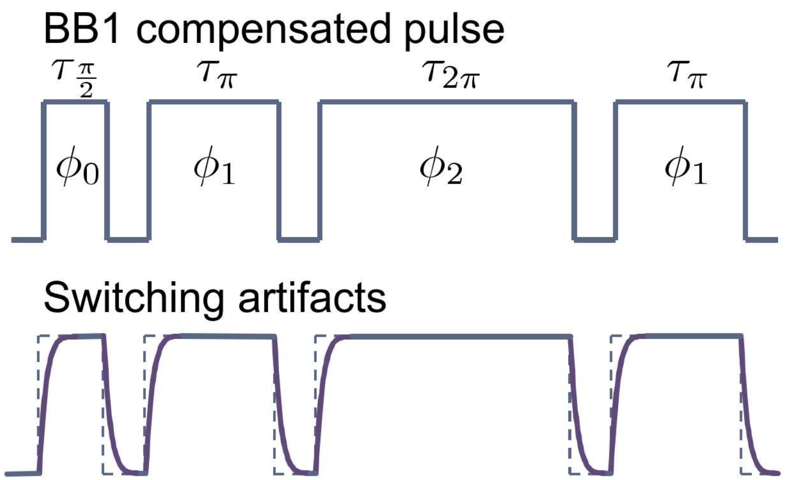

- Calibrate gap offset
- Discontinuous phase updates are used in place of gaps. Solves issues related to finite turn-on time and allows for continuous feedback on the driving field power.

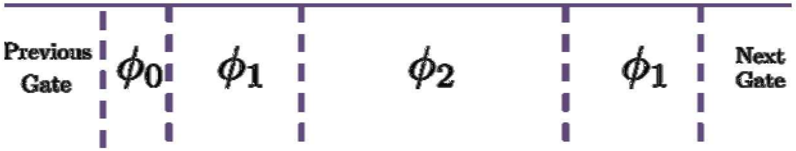

2. BB1 sequence for identity gate

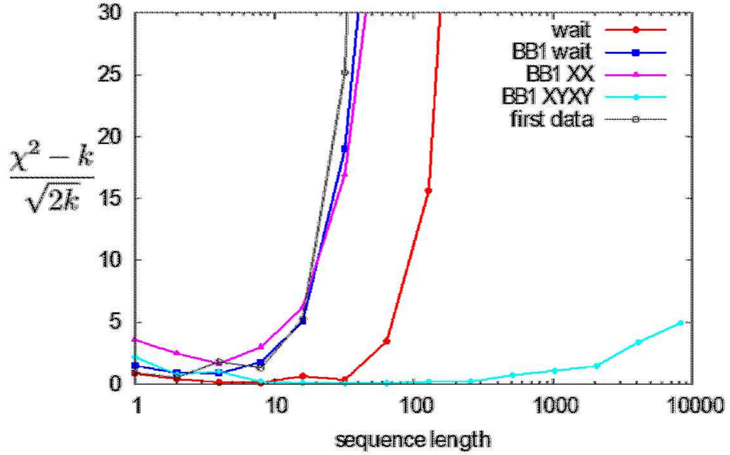

- BB1 decoupled microwave gates with decoupled identity have very small non-Markovian noise
- Decoupling sequence for identity gate
- Drift control for π-time and qubit frequency

Gate	Process Infidelity	1/2 ◇-Norm
G_I	$6.9(6) \times 10^{-5}$	$7.9(7) \times 10^{-5}$
G_X	$6.1(7) \times 10^{-5}$	$7.0(15) \times 10^{-5}$
G_Y	$7.2(7) \times 10^{-5}$	$8.1(15) \times 10^{-5}$

95% confidence intervals

GST – Microwaves (on-chip)

- Off-resonant coupling observed with long RB sequences targeting both qubit states
- Culprit – impurity in polarizations that lead to leakage into the Zeeman states

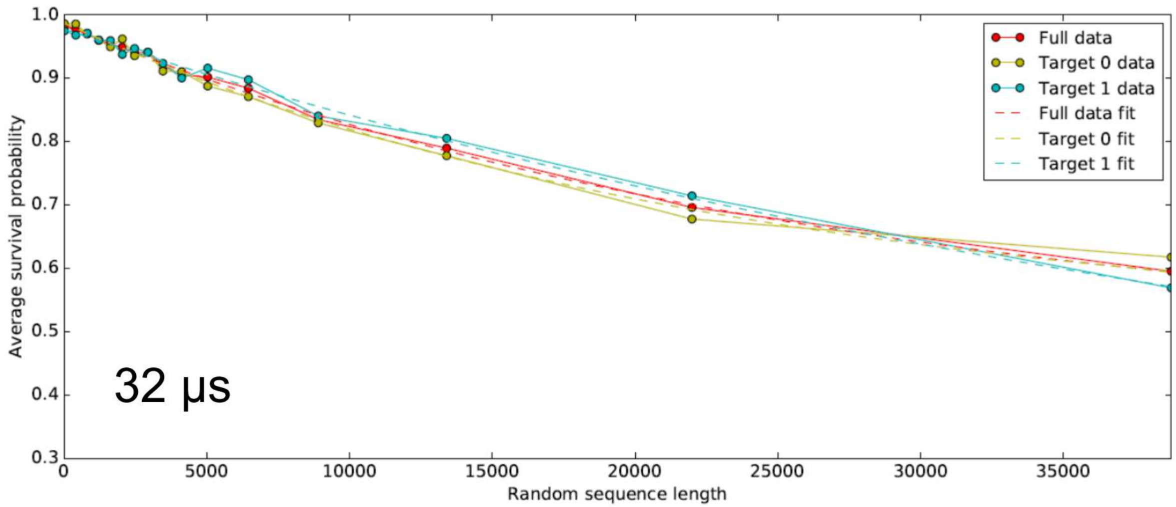

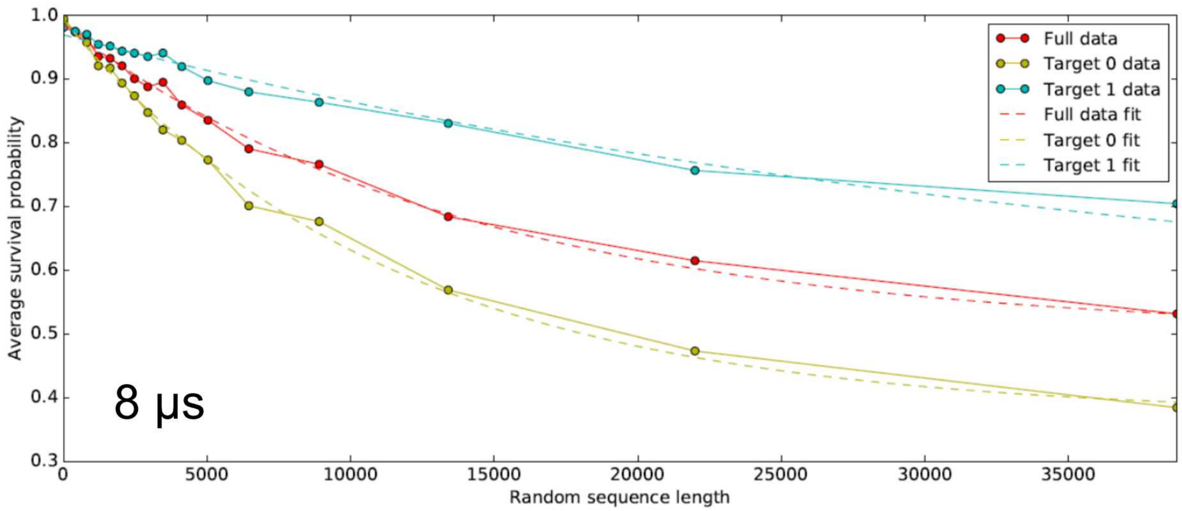

Laser based Raman gates

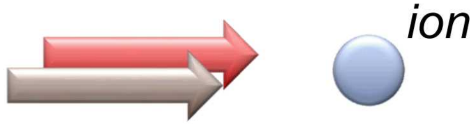

co-propagating beam geometry

- Motion independent
- No optical phase imprinted

- BB1 dynamically compensated pulse sequences

GST results:

95% confidence intervals

	Conventional pulses		Gapless pulses	
Gate	Process Infidelity	½ ◇-Norm	Process Infidelity	½ ◇-Norm
G_I	$0.05(2) \times 10^{-4}$	$12(1) \times 10^{-4}$	$1.1(1) \times 10^{-4}$	$5.3(2) \times 10^{-4}$
G_X	$1.3(1) \times 10^{-4}$	$4(2) \times 10^{-4}$	$0.5(1) \times 10^{-4}$	$2(6) \times 10^{-4}$
G_Y	$1.6(4) \times 10^{-4}$	$4(3) \times 10^{-4}$	$0.7(1) \times 10^{-4}$	$4(9) \times 10^{-4}$

Mølmer-Sørensen gates

- Mølmer-Sørensen gates [1]
- All two-qubit gates implemented using Walsh compensation pulses [2]

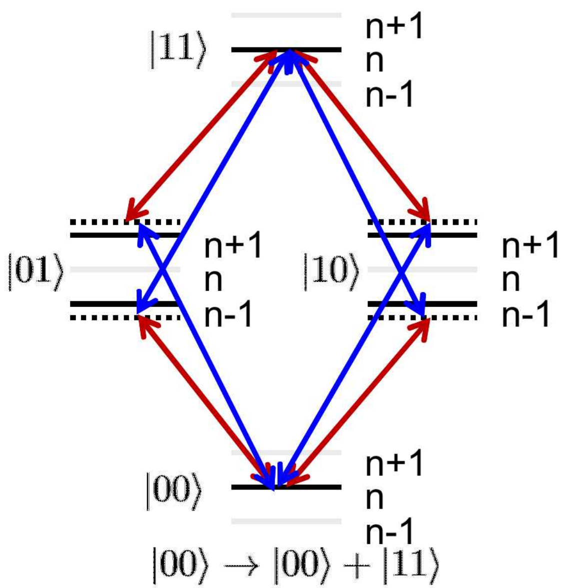

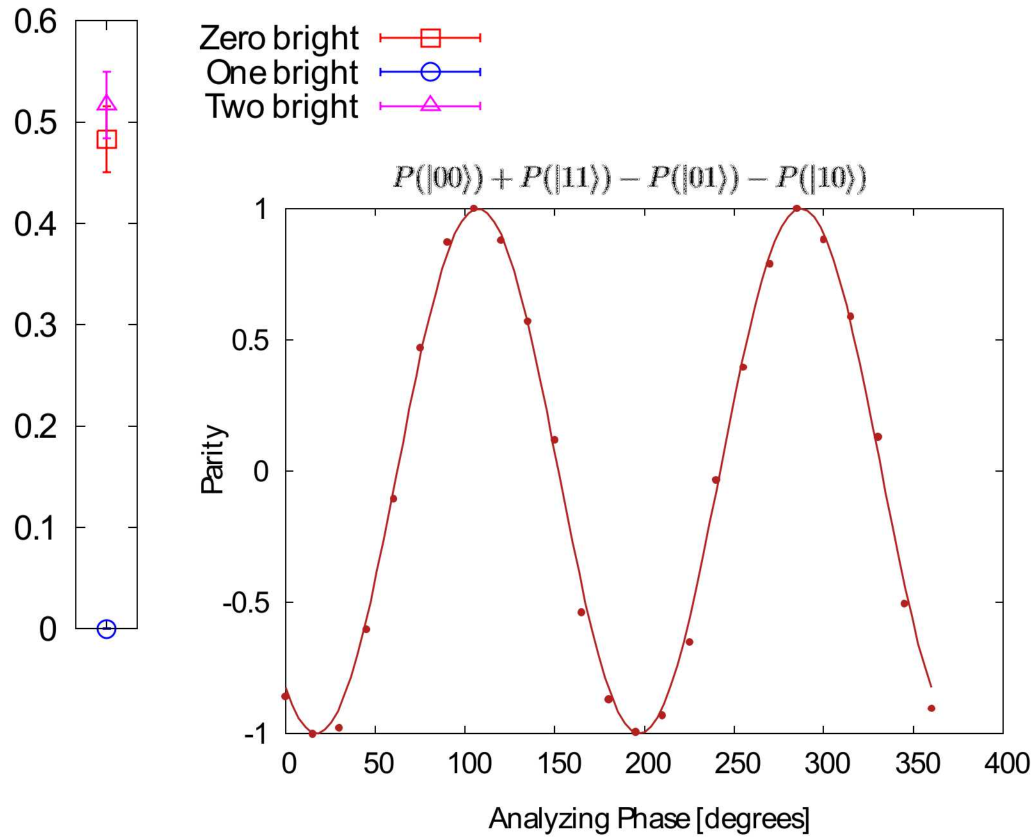

$$\mathcal{F} = \frac{1}{2}(P(|00\rangle) + P(|11\rangle)) + \frac{1}{4}c \approx 0.995$$

[1] K. Mølmer, A. Sørensen, PRL 82, 1835 (1999)

[2] D. Hayes et al. Phys. Rev. Lett. 109, 020503 (2012)

Diagnostics - two qubit gates

GST on symmetric subspace

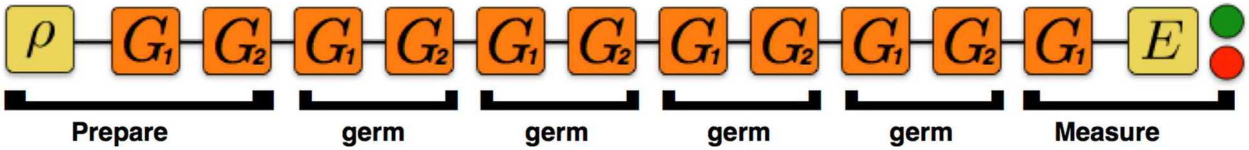

Basic gates:

$$G_I$$

$$G_{XX} = G_X \otimes G_X$$

$$G_{YY} = G_Y \otimes G_Y$$

$$G_{MS}$$

Preparation Fiducials:

$\{\}$

G_{XX}

G_{YY}

G_{MS}

$G_{XX}G_{MS}$

$G_{YY}G_{MS}$

Germs:

G_I

G_{XX}

G_{YY}

G_{MS}

$G_I G_{XX}$

$G_I G_{YY}$

$G_I G_{MS}$

$G_{XX}G_{YY}$

$G_{XX}G_{MS}$

$G_{YY}G_{MS}$

$G_I G_I G_{XX}$

$G_I G_I G_{YY}$

Detection Fiducials:

$\{\}$

G_{XX}

G_{YY}

G_{MS}

$G_{XX}G_{MS}$

$G_{YY}G_{MS}$

G_{XX}^3

G_{YY}^3

$G_{YY}^2 G_{MS}$

GST on symmetric subspace

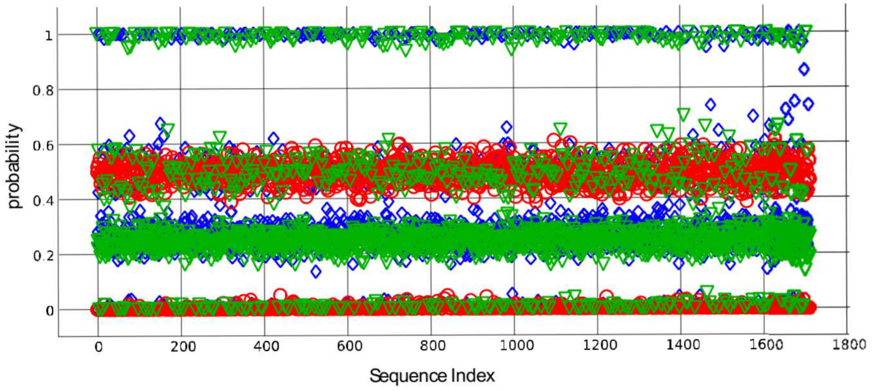

Zero ions bright
One ion bright
Two ions bright

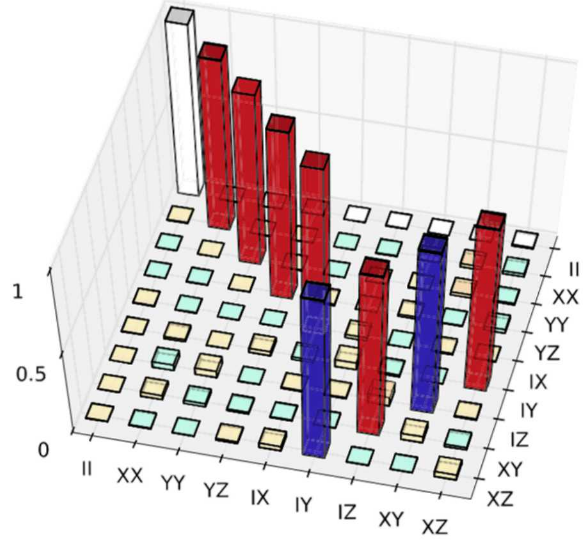

Gate	Process infidelity	$\frac{1}{2}$ Diamond norm
G_I	$1.6 \times 10^{-3} \pm 1.6 \times 10^{-3}$	$28 \times 10^{-3} \pm 7 \times 10^{-3}$
G_{XX}	$0.4 \times 10^{-3} \pm 1.0 \times 10^{-3}$	$27 \times 10^{-3} \pm 5 \times 10^{-3}$
G_{YY}	$0.1 \times 10^{-3} \pm 0.9 \times 10^{-3}$	$26 \times 10^{-3} \pm 4 \times 10^{-3}$
G_{MS}	$4.2 \times 10^{-3} \pm 0.6 \times 10^{-3}$	$38 \times 10^{-3} \pm 5 \times 10^{-3}$

95% confidence intervals

Process fidelity of two-qubit Mølmer-Sørensen gate > 99.5%

Summary

Leveraging DOE facilities

- MESA facility – capabilities align well with trap requirements
  - Engineers and technologists essential to fabricating and packaging the many traps needed at SNL and academic/commercial partners
- Engineering and simulations
  - Microwave design
  - Quantum theory – tomography and error correction
- LDRD support (primary support from IARPA)

Future research

- Ion transport to support logical qubit operations
- Continue to improve fidelity in context of logical qubits

Postdoc positions available

Trap design and fabrication
Matthew Blain
Ed Heller
Corrie Herrmann
Becky Loviza
John Rembetski
Paul Resnick
SiFab team

Trap packaging
Ray Haltli
Drew Hollowell
Anathea Ortega
Tipp Soumphonphakdy

GST protocols
Robin Blume-Kohout
Kenneth Rudinger
Eric Nielsen

Trap design and testing
Peter Maunz
Craig Hogle
Daniel Lobser
Melissa Revelle
Dan Stick
Christopher Yale

RF Engineering
Christopher Nordquist
Stefan Lepkowski

Backup slides

Microwave error sources

- Time resolution:
  - Current time resolution is 5 ns
  - π-times are 45 μs
  - ratio: 10^{-4}
  - Possible due to broadband pulses
- Coherence time:
  - $T_2^* = 1\,\mathrm{s}$
  - longest pulse sequences 8192 : 1.66 s

Transport

$$\mathcal{H} = \begin{pmatrix} \frac{\partial\phi}{\partial x\partial x} & \frac{\partial\phi}{\partial x\partial y} & \frac{\partial\phi}{\partial x\partial z} \\ \frac{\partial\phi}{\partial y\partial x} & \frac{\partial\phi}{\partial y\partial y} & \frac{\partial\phi}{\partial y\partial z} \\ \frac{\partial\phi}{\partial z\partial x} & \frac{\partial\phi}{\partial z\partial y} & \frac{\partial\phi}{\partial z\partial z} \end{pmatrix}$$

- Symmetric curvature tensor
- 6 degrees of freedom
- Determines trap frequencies and principal axes rotations
- Traceless for static fields
- Trace is generated by rf pseudopotential

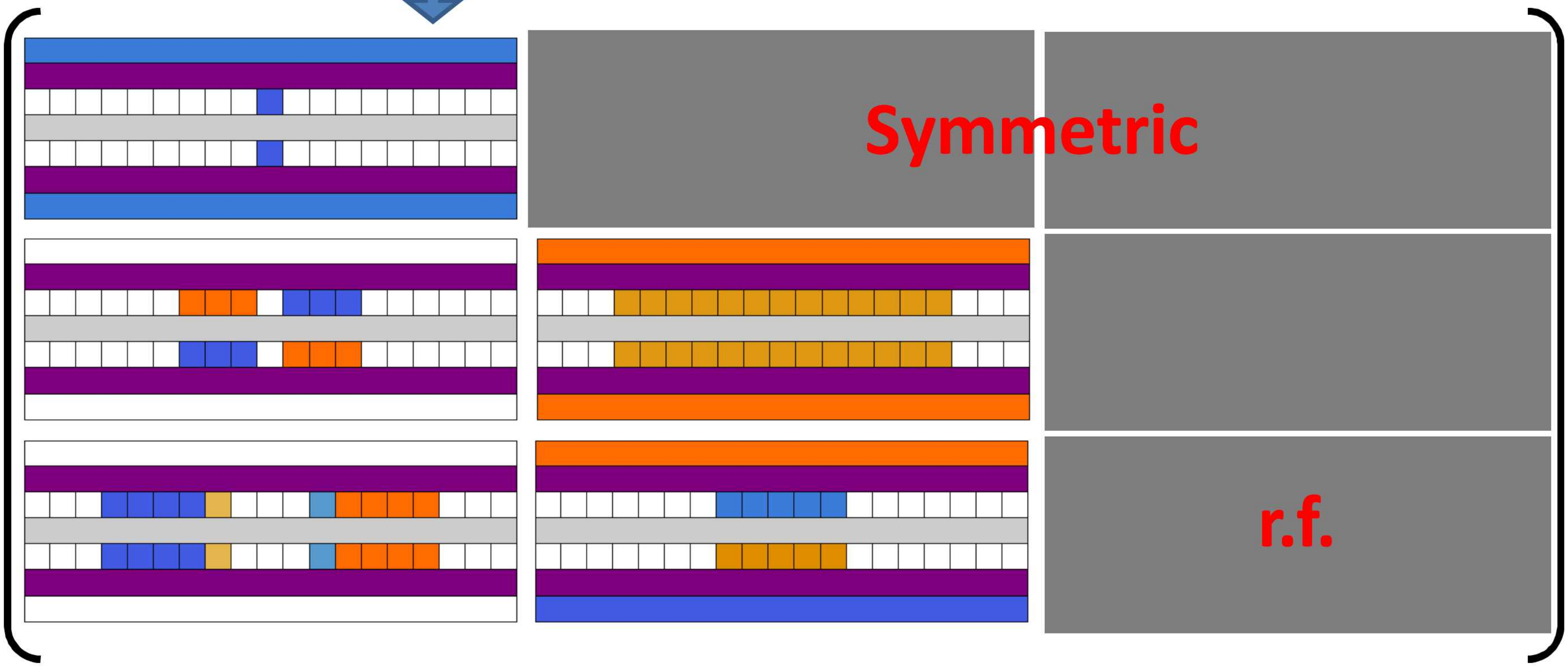

Voltage application

Trapping potential

- Axial frequency: 500 kHz [<5 V]
- Radial frequency: 2.8 MHz, 3.1 MHz [250 Vrf @ 40 MHz]

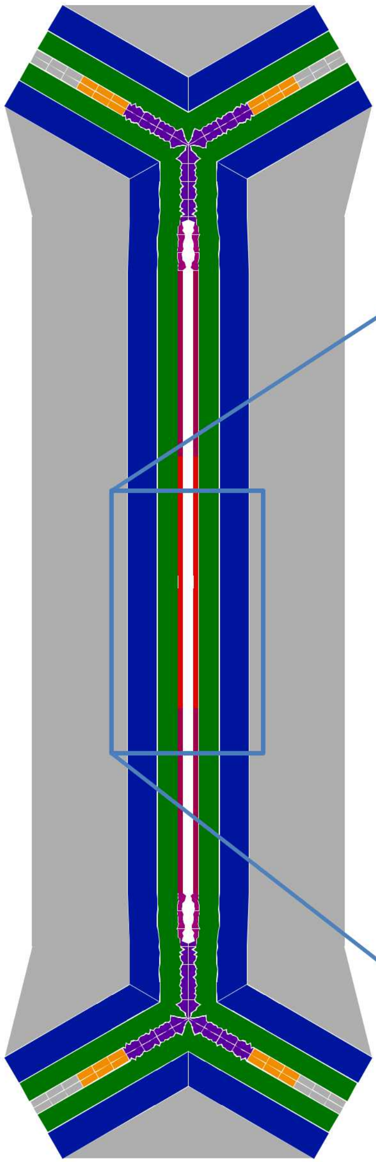

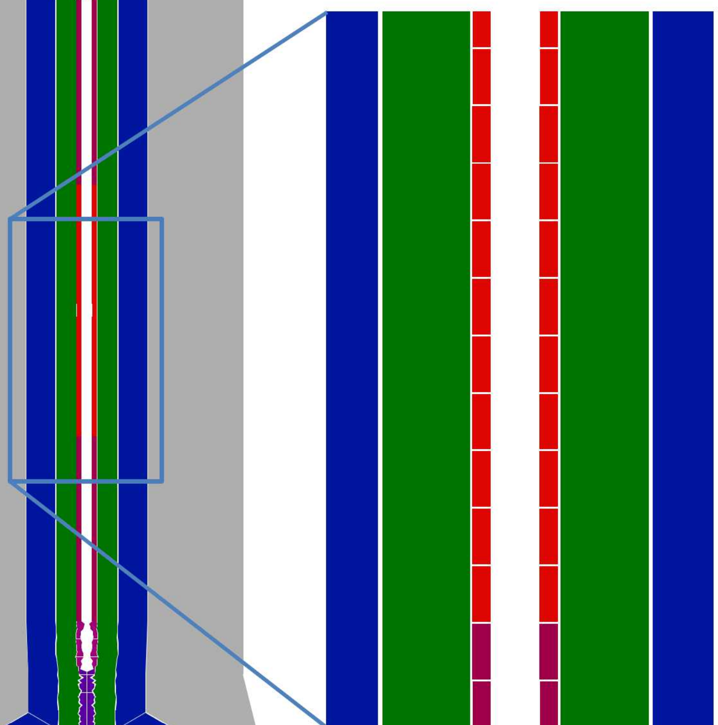

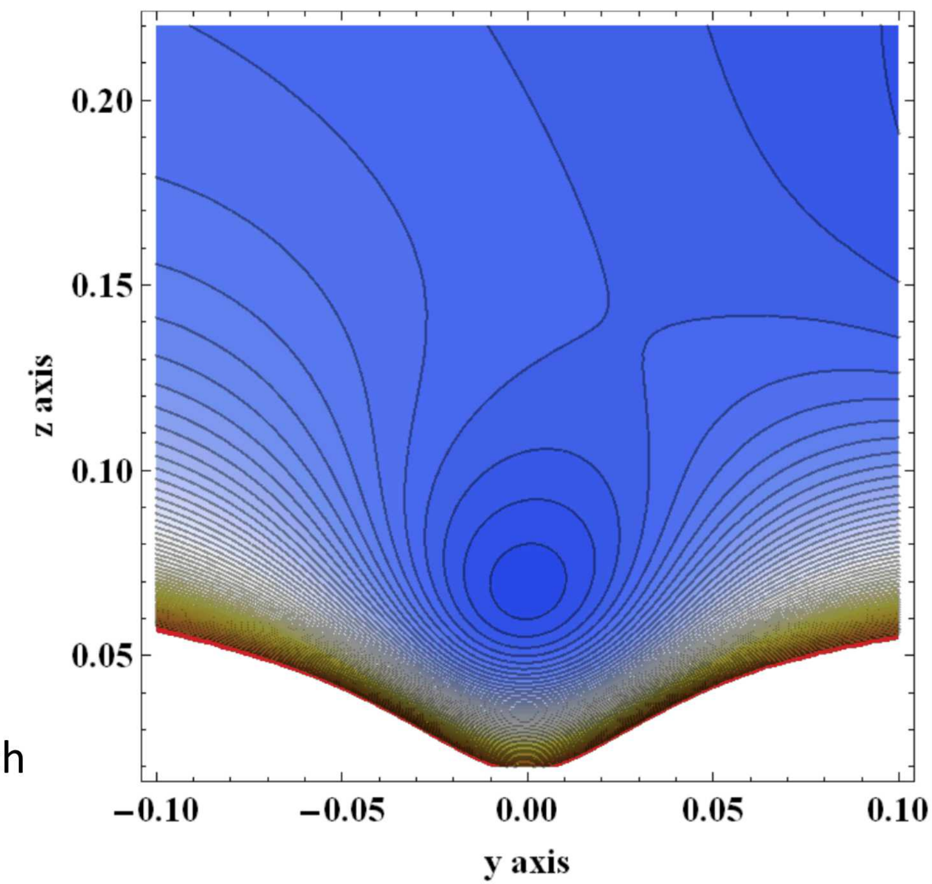

- 70 µm electrode pitch
- 70 µm ion height

Microwave surface trap

“Ideal” Two-Loop Design

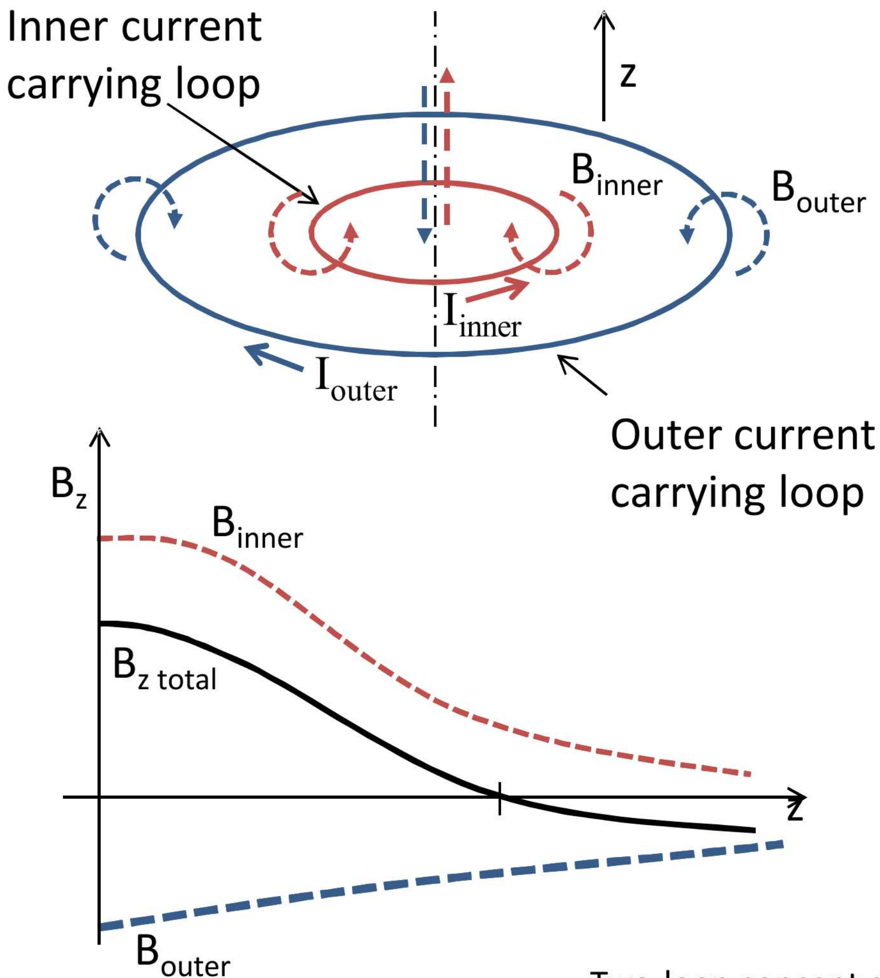

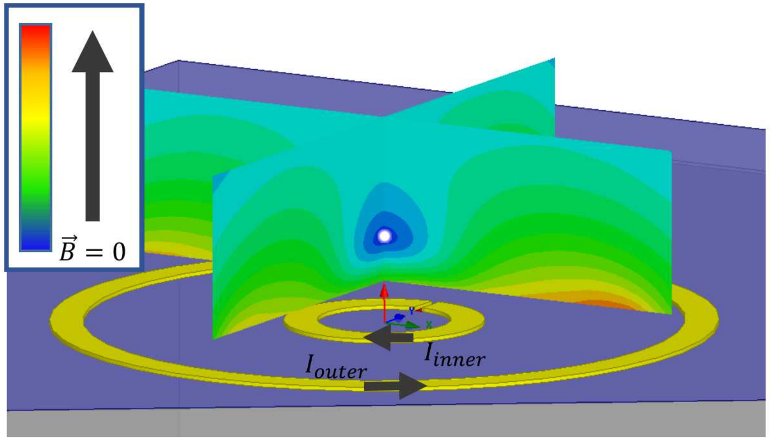

- x- and y- fields cancel along z-axis
- Generates uniform Bz and dBz/dz with B=0
- Location of null determined by geometry and ratio of currents

Two-loop concept developed at Sandia in 2012 (SAND2015-9513)
(C. Highstrete, S. M. Scott, J. D. Sterk, C. D. Nordquist, J. E. Stevens, C. P. Tigges, M. G. Blain)

Trap fabrication capability

- Any geometry can be realized
  - Islanded electrodes
  - Clusters of small electrodes
  - Segmented electrodes close to trapping location
- Any (reasonable) shape can be realized
  Example: Bowtie shape for increased numerical aperture
  - 4μm focus possible (@ 370nm)
  - Numerical Aperture 0.1
- Electrodes on different metal levels are possible
- Enables scalability (Quantum-CCD)
- Uses capabilities exceeding CMOS-7 (remove dielectrics, trap shape)

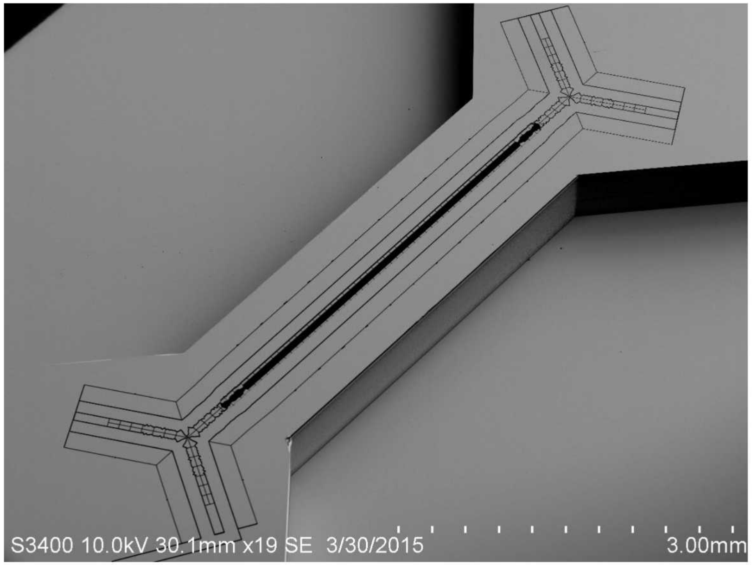

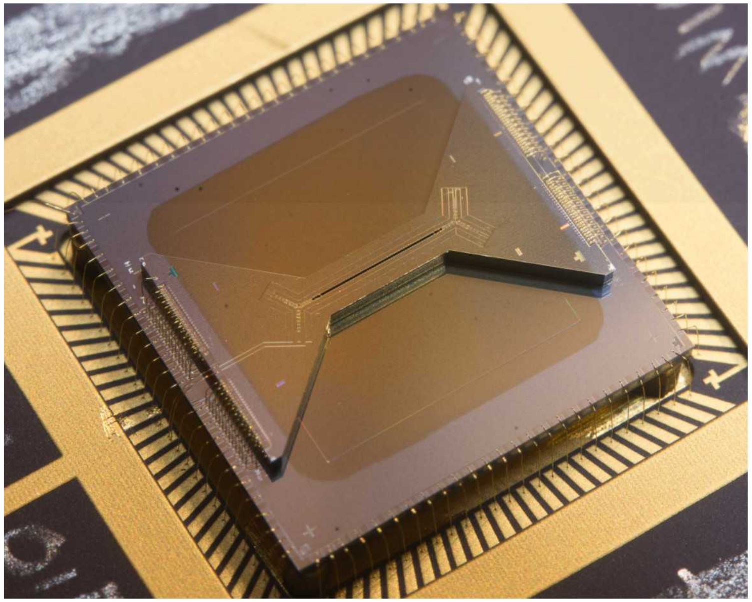

Primitives for scalable devices

Junctions enable 2-D scaling of ion traps

- Fabricated and demonstrated in multiple traps

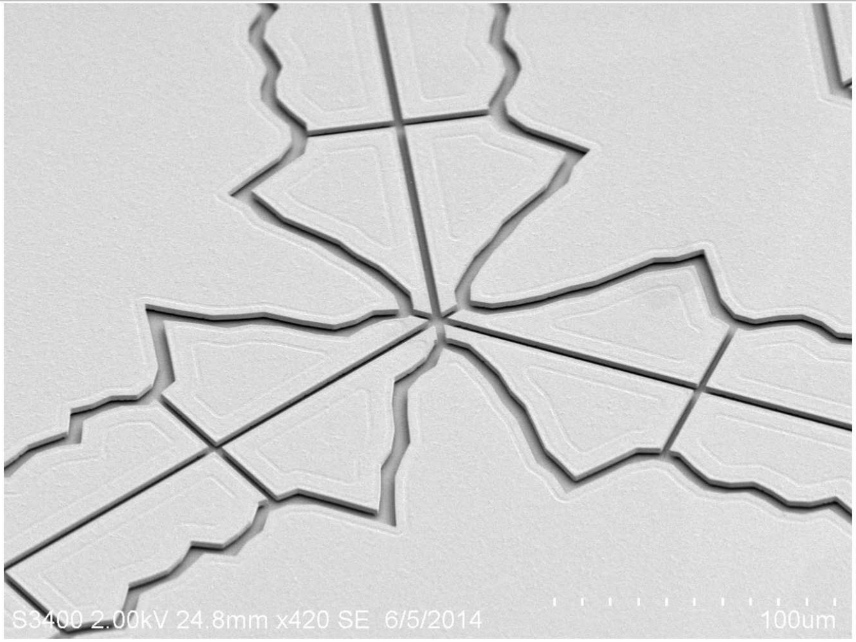

Slotted trapping regions

- Optical access (NA 0.25)
  Enables focus 2μm (@370nm)
- Transitions to above surface necessary to integrate junctions and scale traps
- Modulations reduce pseudopotential bumps to <4meV

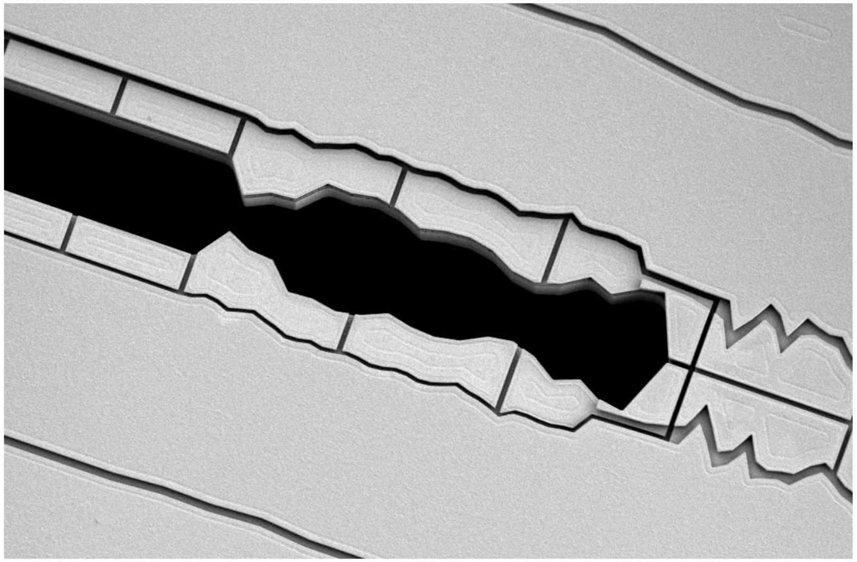

Device Packaging

Why have a packaging standard?

- Plug and trap package
    - Compatible with chambers of many groups
    - Standardized packaging and testing

Packaging developments

- Automatic wirebonding
    - Small pitch possible
    - Improved yield
- Electrical shorts and capacitance test
- Parametric verification (opens test)
- Known good trap
    - Easy deployment
    - Anyone who tried to trap succeeded

We deliver known good devices

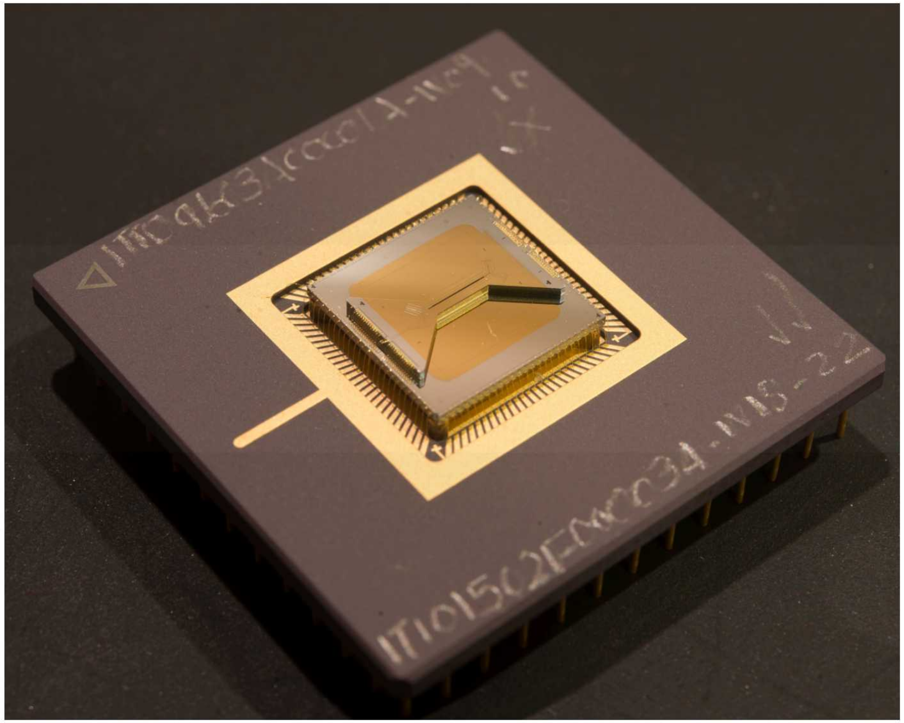

Parametric verification

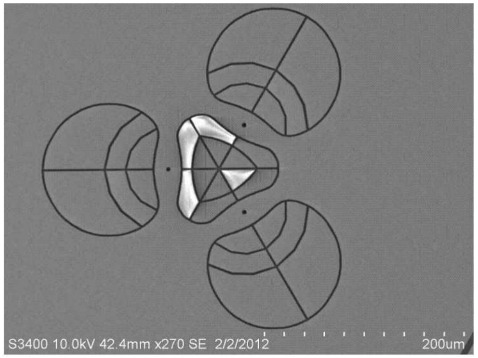

Shuttling in surface traps

- Remaining solutions compensate for micromotion → should produce no curvature

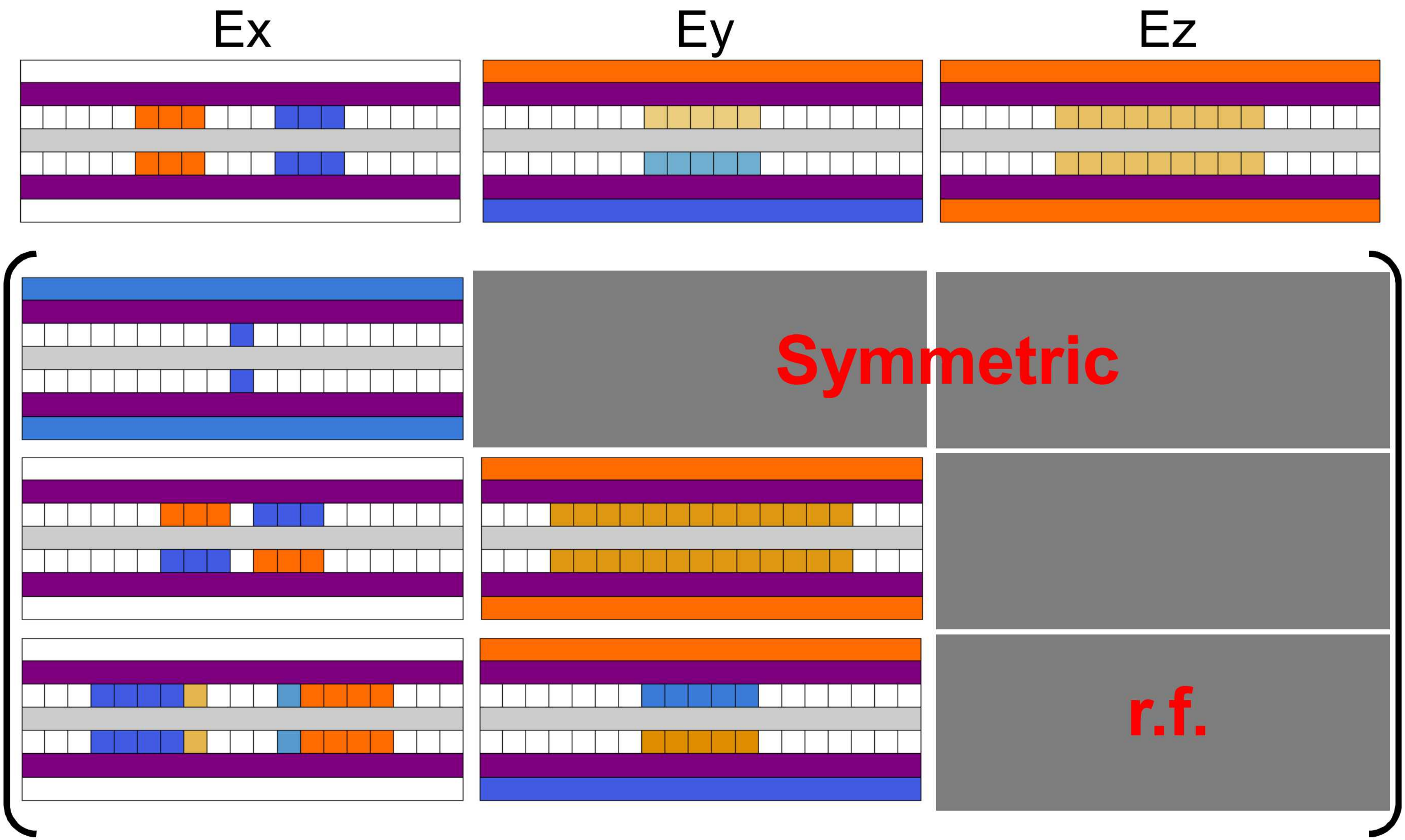

Parametric Rotation Amplitudes

$e_x,\ e_y,\ e_z$: Eigenvalues

$\partial_{xx}\phi$

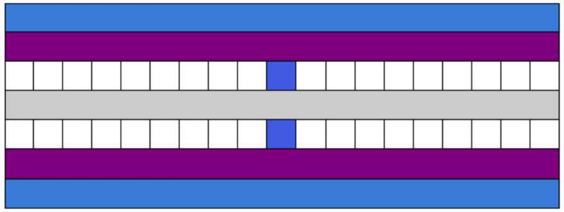

$$e_y \sin^2(\alpha) + e_x \cos^2(\alpha)$$

$\partial_{xy}\phi$

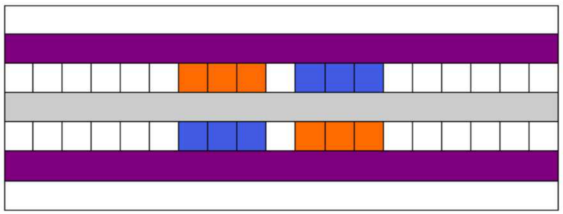

$$(e_y - e_x) \sin(\alpha) \cos(\alpha) \cos(\beta)$$

$\partial_{xz}\phi$

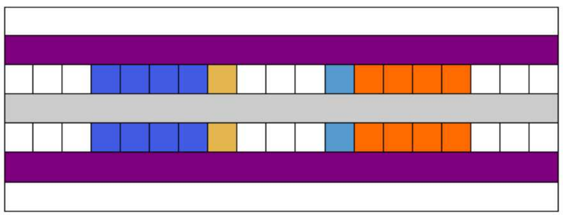

$$(e_x - e_y) \sin(\alpha) \cos(\alpha) \sin(\beta)$$

$\partial_{yy}\phi$

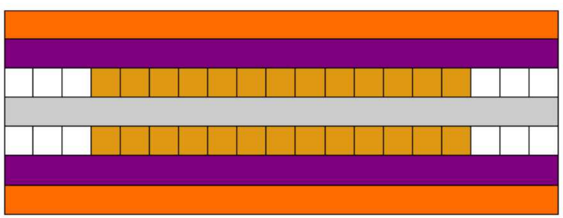

$$\left(\cos^2(\beta) - \sin^2(\beta)\right) \left(e_x \sin^2(\alpha) + e_y \cos^2(\alpha)\right) + \ e_z \sin^2(\beta) - e_z \cos^2(\beta)$$

$\partial_{yz}\phi$

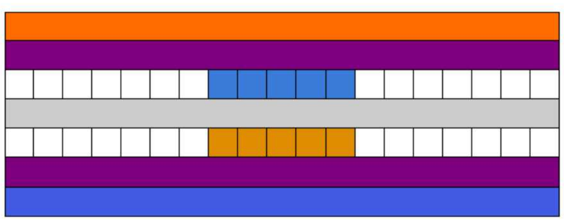

$$\sin(\beta) \cos(\beta) \left(-e_x \sin^2(\alpha) - e_y \cos^2(\alpha) + e_z\right)$$

Rotation of chains
experimental realization

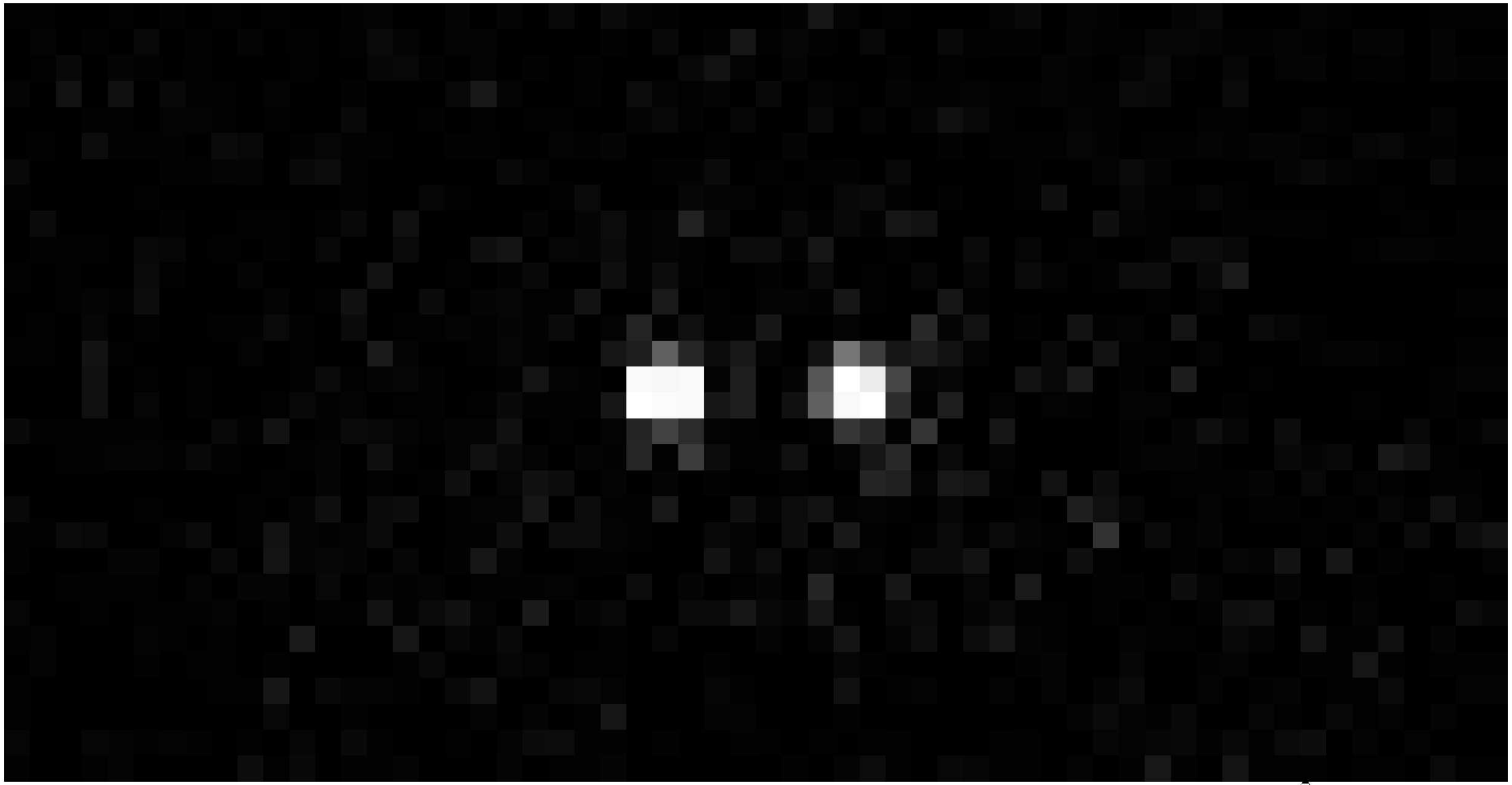

To be characterized as function of swapping time

- Swapping fidelity
- Accumulated motion

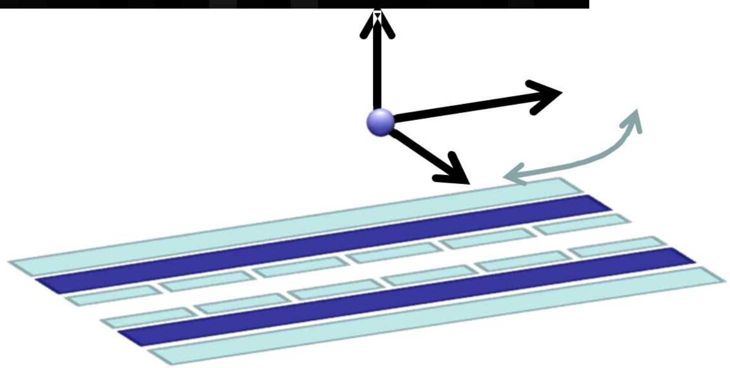

Trap frequency vs linear offset

- Trap frequencies are stable to within 16 kHz over the course of linear shuttling

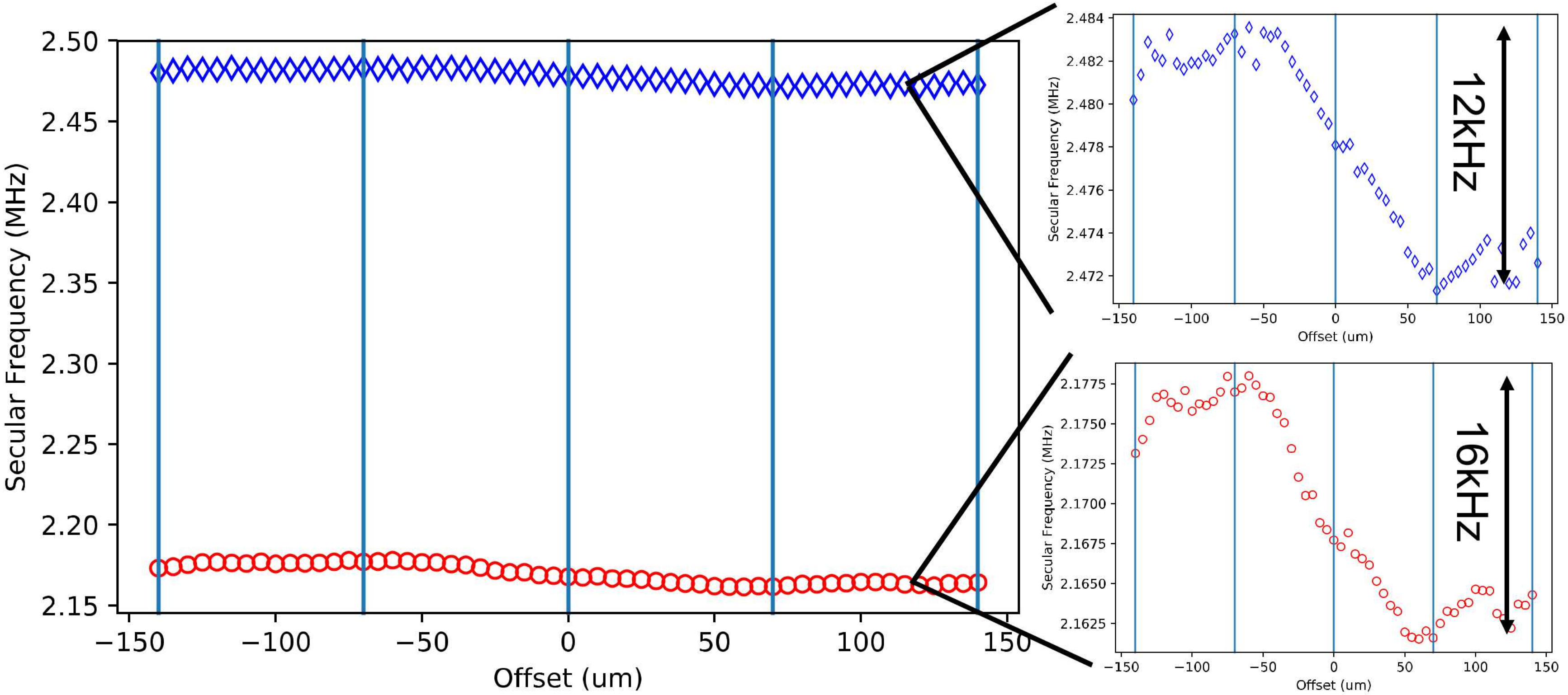

Conclusion

Sandia microfabricated surface traps are ready for your high fidelity operations

Demonstrated:

- Long lifetime, observed ion > 100h
- High fidelity microwave single qubit gates
  Process infidelity $7.2(7) \times 10^{-5}$
  below fault tolerance threshold $\frac{1}{2}\,\|\cdot\|_{\diamond} = 8(1) \times 10^{-5}$
- High fidelity Raman laser single qubit gates
  Process infidelity 1.6×10^{-4} $\frac{1}{2}\,\|\cdot\|_{\diamond} = 5.3(2) \times 10^{-4}$
- High fidelity two qubit gates
  Process infidelity $4.2(6) \times 10^{-3}$ $\frac{1}{2}\,\|\cdot\|_{\diamond} = 38(5) \times 10^{-3}$

Swapping fidelity

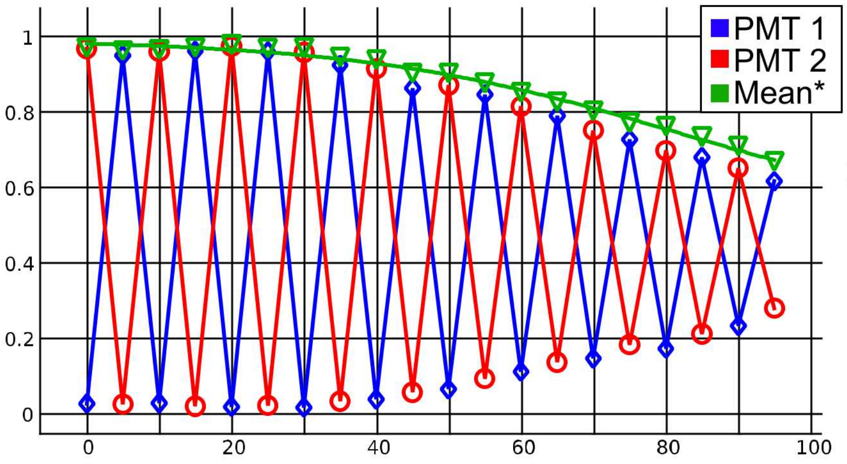

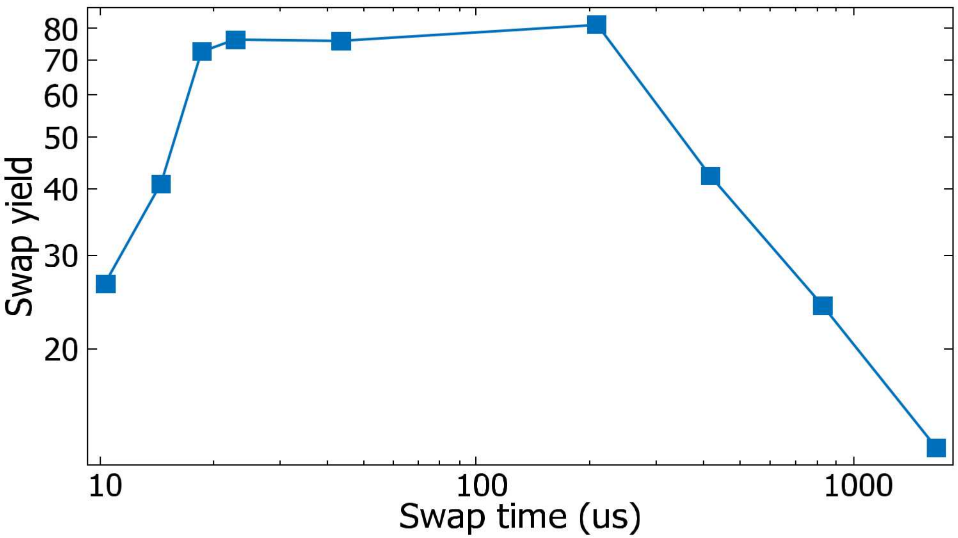

- Best fidelity between 20μs and 200μs
- Failure probability increases with number of swaps (heating)

Gate Set Tomography

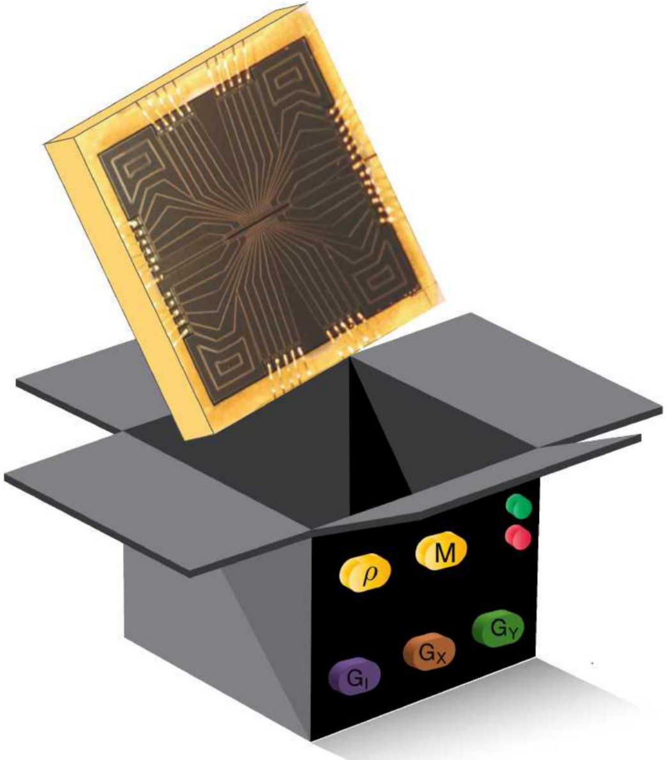

Developed at Sandia by
QCVV team

- No calibration required
- Detailed debug information
- Efficiently measures performance characterizing fault-tolerance (diamond norm)
- Detects non-Markovian noise

Uses structured sequences to amplify all possible errors

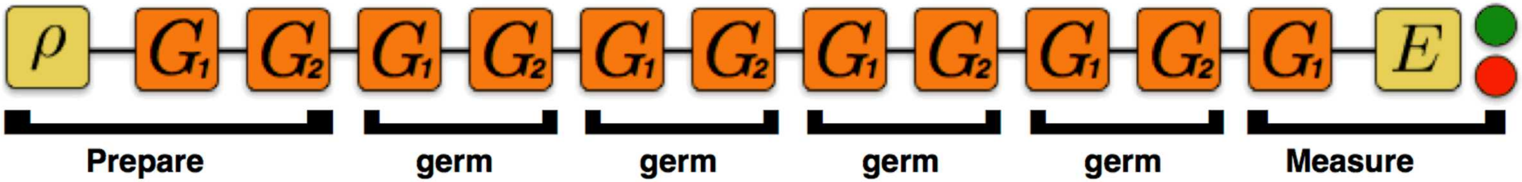

GST Experiments

Single qubit BB1 compensated microwave gates on $^{171}Yb^{+}$

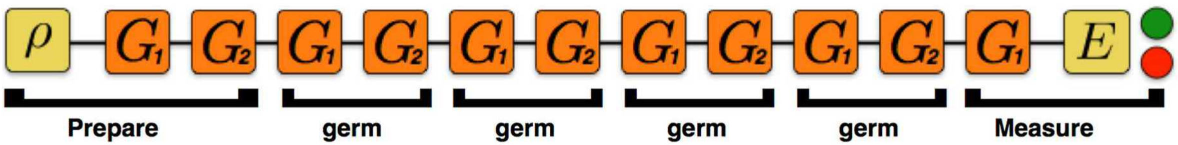

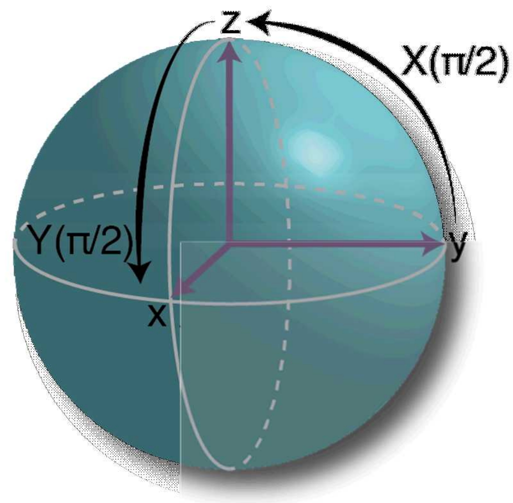

Desired "target" gates:

G_i Idle (Identity)

G_x $\pi/2$ rotation about x-axis

G_y $\pi/2$ rotation about y-axis

Fiducials:

$$\{\}$$
$$Gx$$
$$Gy$$
$$Gx \cdot Gx$$
$$Gx \cdot Gx \cdot Gx$$
$$Gy \cdot Gy \cdot Gy$$

Approximately prepare 6 points on Bloch sphere

Ge

$$Gi$$
$$Gx \cdot Gy$$
$$Gx \cdot Gy \cdot Gi$$
$$Gx \cdot Gi \cdot Gy$$
$$Gx \cdot Gi \cdot Gi$$
$$Gy \cdot Gi \cdot Gi$$
$$Gx \cdot Gx \cdot Gi \cdot Gy$$
$$Gx \cdot Gy \cdot Gy \cdot Gi$$
$$Gx \cdot Gx \cdot Gy \cdot Gx \cdot Gy \cdot Gy$$

Context and time dependency of gates

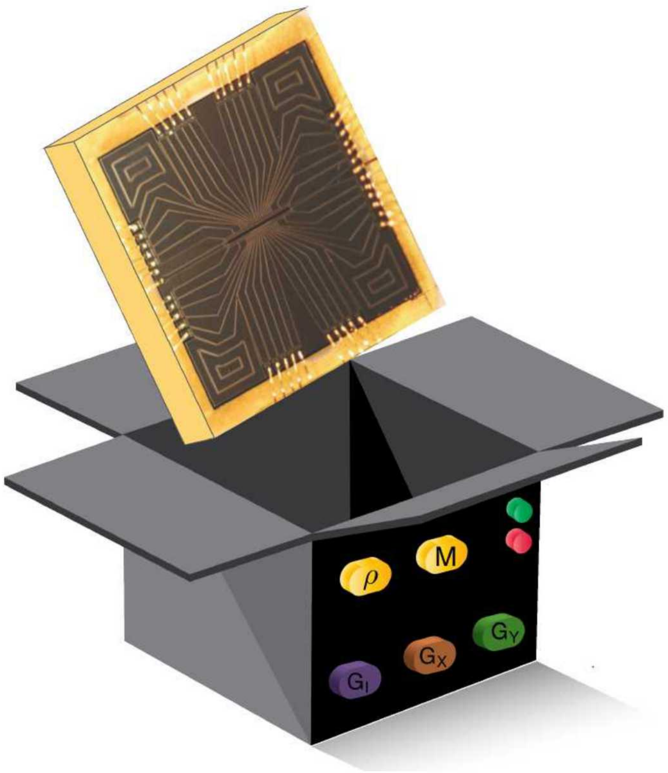

Assumptions:
- Qubits in a box
- Pressing a button always executes the exactly same operation
- Independent from context (gates executed before)
- Independent from when a gate is executed

GST uses a large (over-complete) number of sequences.

We can look whether the assumptions are satisfied

Ongoing work to improve and distinguish detection of context and time dependence of classical control

The Ytterbium Qubit

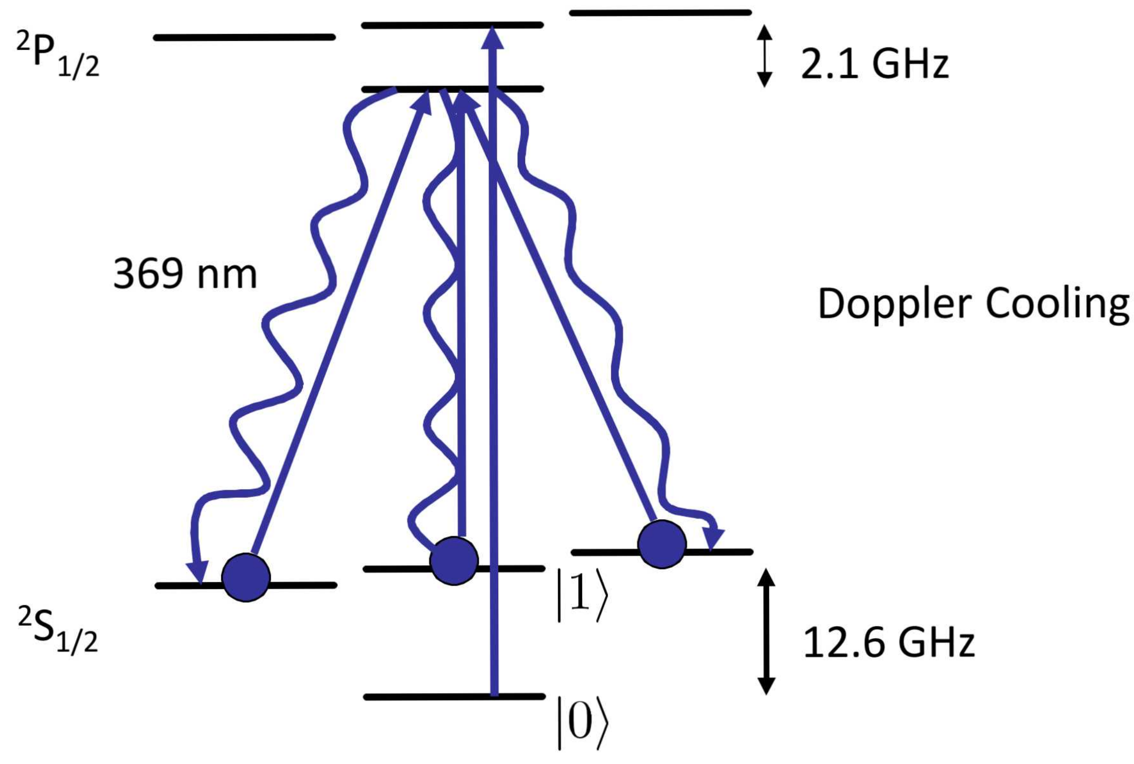

clock state qubit, magnetic field insensitive.

S. Olmschenk *et al.*, PRA **76**, 052314 (2007)

state initialization

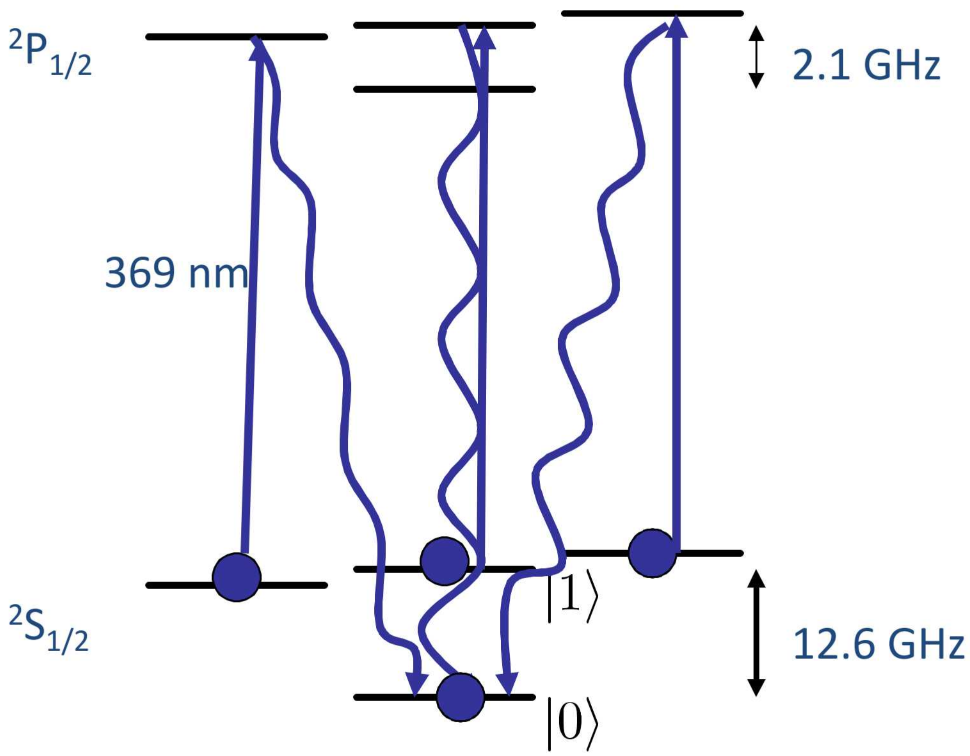

clock state qubit, magnetic field insensitive.

S. Olmschenk *et al.*, PRA **76**, 052314 (2007)

$^{171}Yb^{+}$ state detection

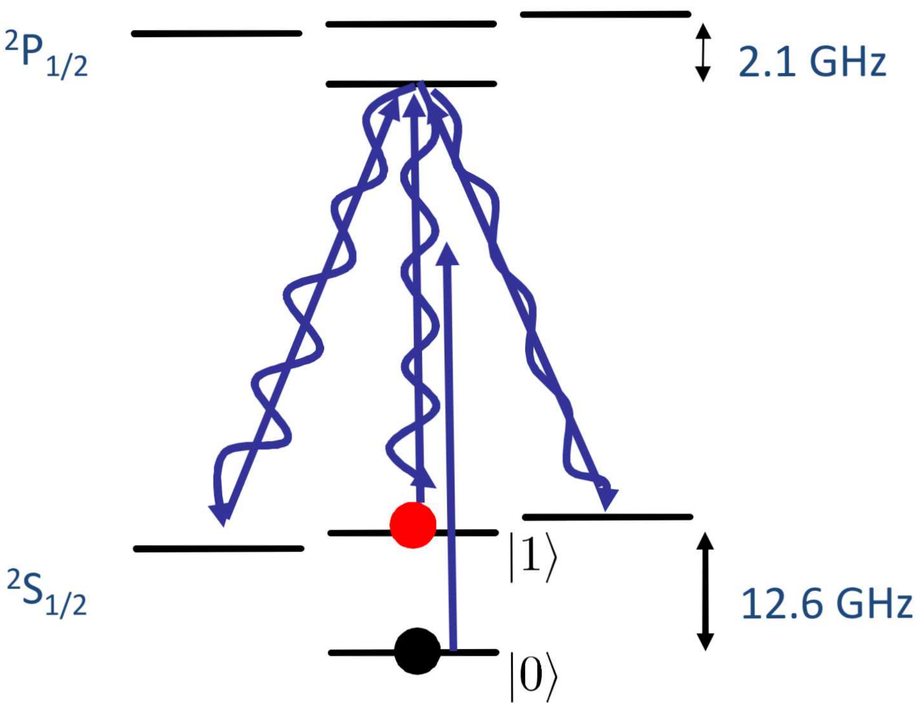

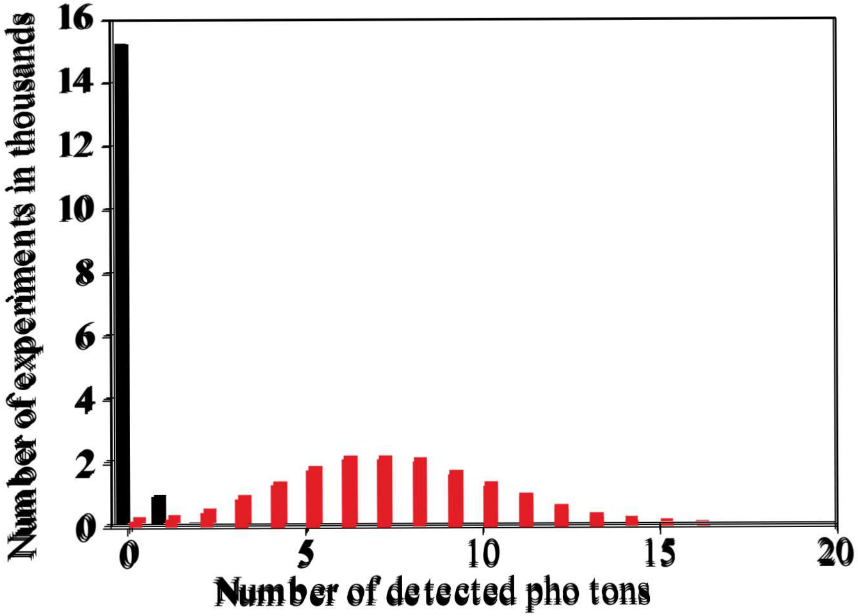

S. Olmschenk *et al.*, PRA **76**, 052314 (2007)

Swapping fidelity

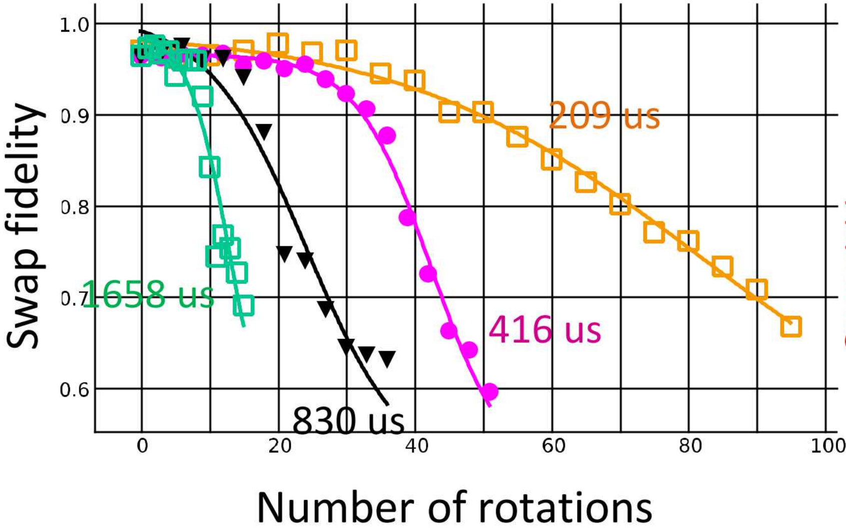

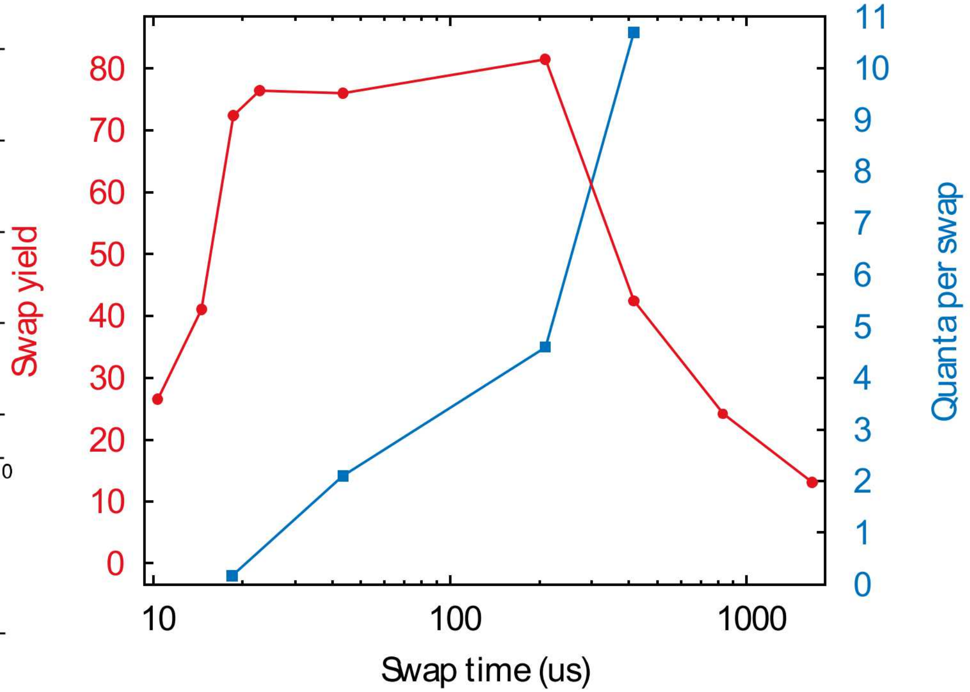

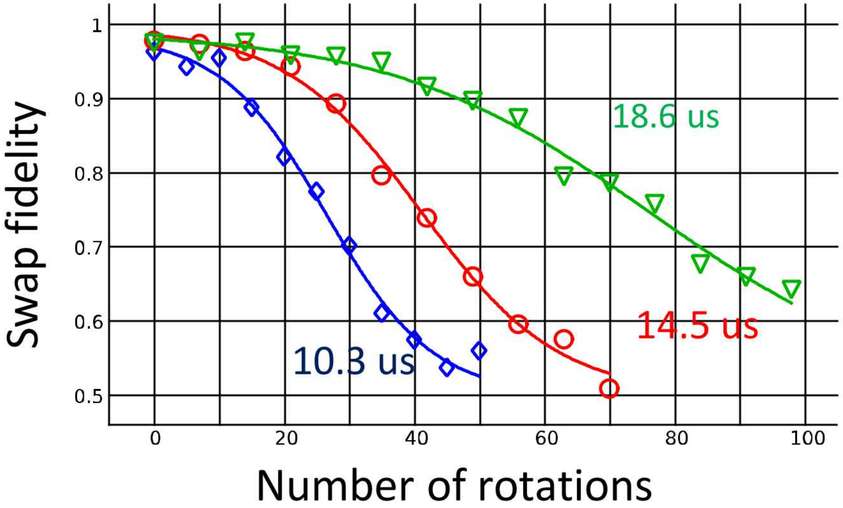

- Best fidelity between 20μs and 200μs
- Failure probability increases with number of swaps (heating)

HOA-2 heating rates

$^{171}Yb^{+}$, Trap frequency 2.8 MHz, r.f. 50 MHz

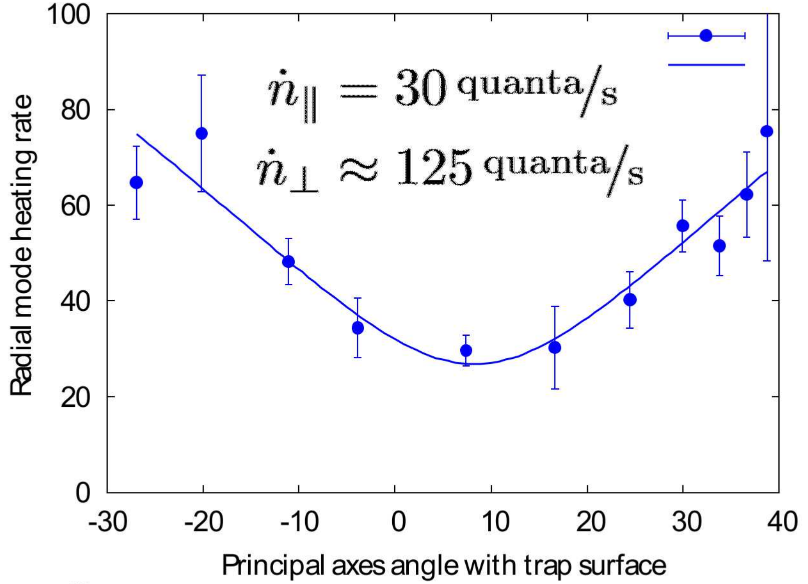

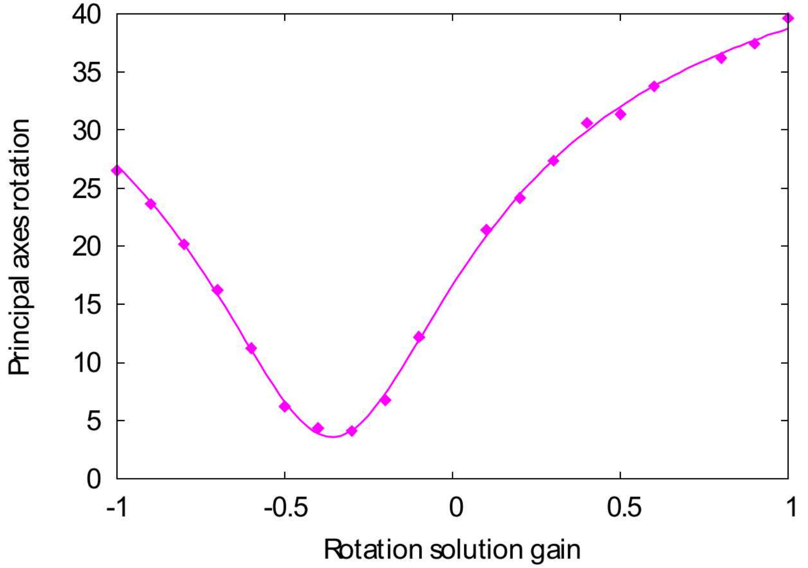

Heating rates as function of principal axes rotation

- Principal axes rotation measured by measuring π-times of Rabi flopping on cooled motional modes
- Minimal heating rates for motional mode parallel to trap surface $\dot{n}_{\parallel}$
- Without technical noise: Vertical mode has at most $\dot{n}_{\perp} \leq 2\dot{n}_{\parallel}$

  (P. Schindler, et al., Phys. Rev. A **92**, 013414 (2015).
- Limited by technical noise

Process fidelity of two-qubit gate

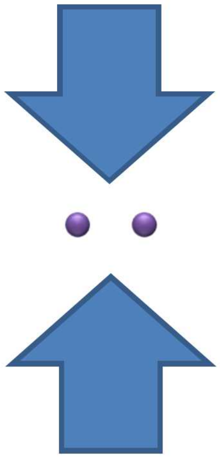

Currently:

- Two ions in single trap well
- No individual addressing

- Ideally all operations are symmetric
- Only symmetric subspace of two-qubit Hilbert space is accessible

Solution:
Perform GST on symmetric subspace
of two-qubit Hilbert space

Fundamental gates:

$$G_I$$

$$G_{XX} = G_X \otimes G_X$$

$$G_{YY} = G_Y \otimes G_Y$$

$$G_{MS}$$

9 Preparation Fiducials
12 Germs
6 Measurement Fiducials:

Linear chain melting

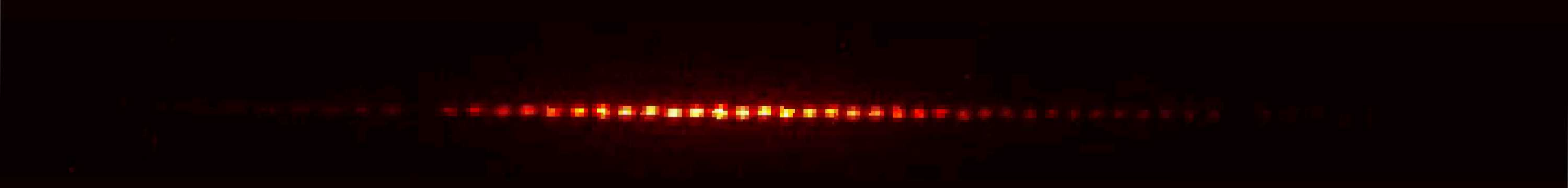

Slightly buckled chain stability

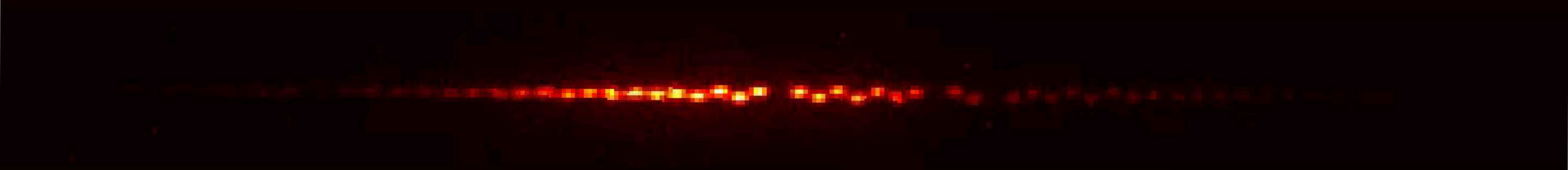

Ramping up buckling

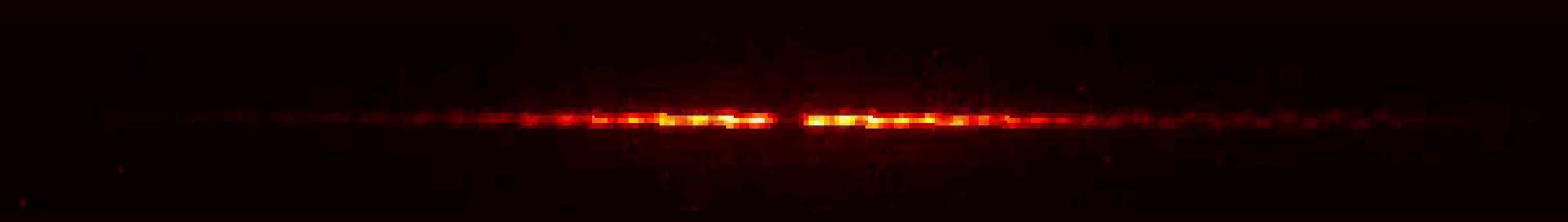

Ion "braid" stability

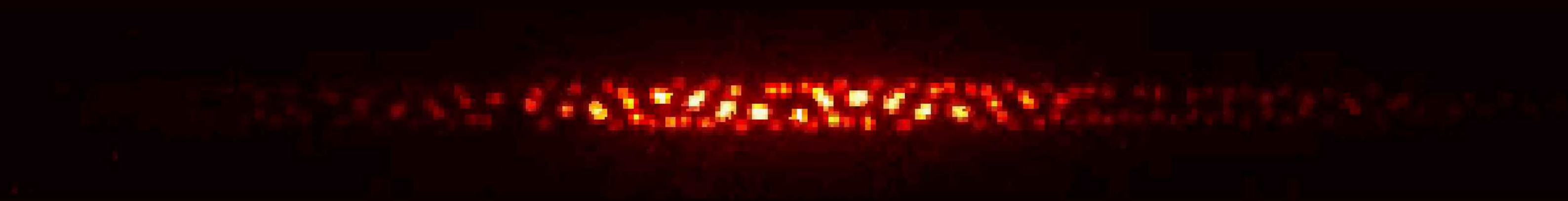

Compression of ion chains

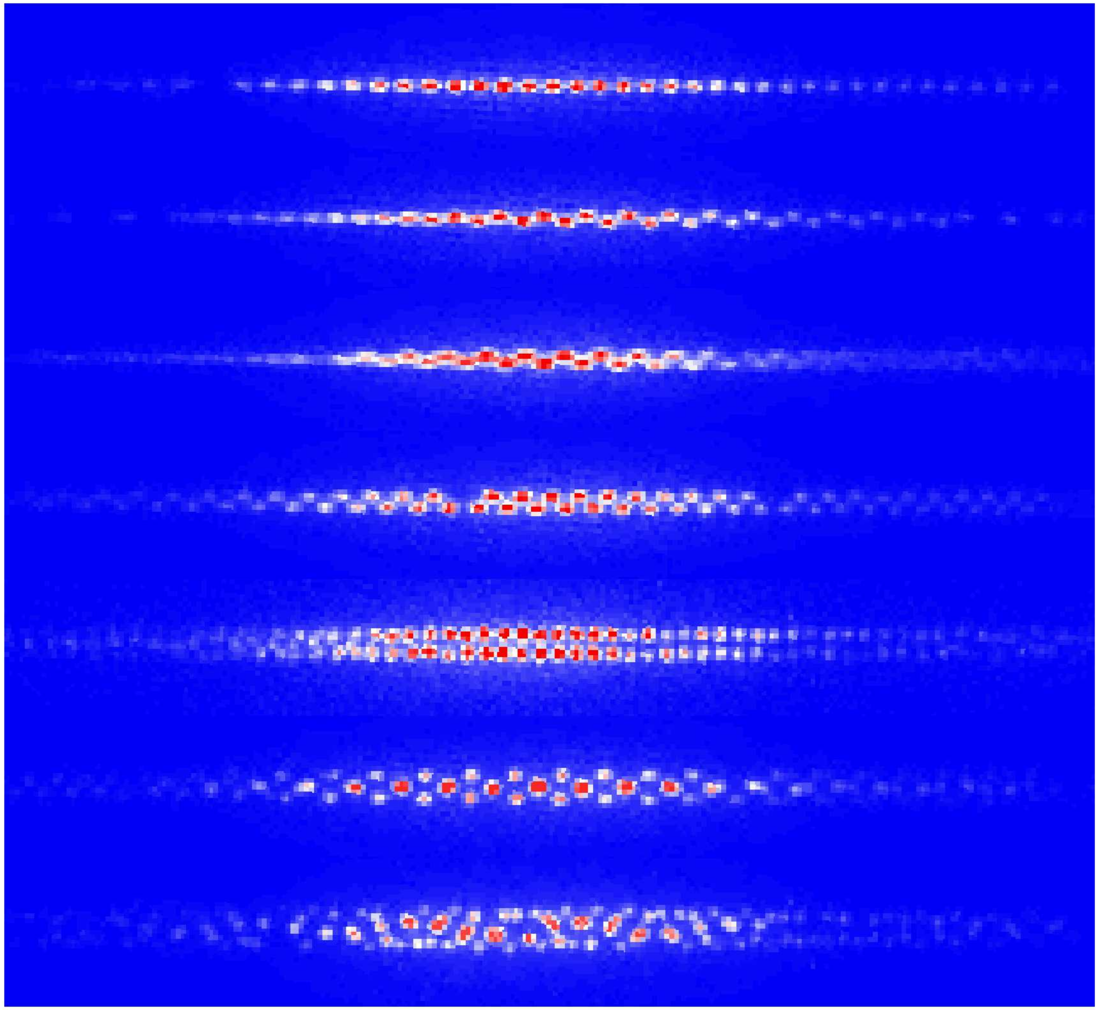

lifetime

15 min

1.5 hours

> 16 hours